IFT

Instituto de Física Teórica
Universidade Estadual Paulista

Ph.D. THESIS / TESE DE DOUTORAMENTO IFT-T.003/18

Electron and muon anomalous magnetic dipole moment in the 3-3-1 model with heavy leptons

O momento de dipolo magnético anômalo do elétron e do múon no modelo 3-3-1 com léptons pesados

George De Conto Santos

Advisor / Orientador

Vicente Pleitez

March 2018 / Março de 2018

Acknowledgements

I would like to thank Conselho Nacional de Desenvolvimento Científico e Tecnológico (CNPq) for the financial support. Also would like to thank Instituto de Física Teórica - Universidade Estadual Paulista (IFT-UNESP) for the opportunity, infrastructure and support to realize this work.

More importantly, I would like to thank Prof. Vicente Pleitez for his supervision, time, effort and support.

Abstract

We calculate, in the context of the 3-3-1 model with heavy charged leptons, constraints on some parameters of the extra particles in the model by imposing that their contributions to both the electron and muon $(g-2)$ factors are in agreement with experimental data up to 1σ-3σ. In order to obtain realistic results we use some of the possible solutions of the left- and right- unitary matrices that diagonalize the lepton mass matrices, giving the observed lepton masses and at the same time allowing to accommodate the Pontecorvo-Maki-Nakagawa-Sakata (PMNS) mixing matrix. We show that, at least up to 1-loop order, in the particular range of the space parameter that we have explored, it is not possible to fit the observed electron and muon $(g-2)$ factors at the same time unless one of the extra leptons has a mass of the order of 20-40 GeVs and the energy scale of the 331 symmetry to be of around 60-80 TeVs.

Keywords: magnetic dipole moment, muon, electron, 3-3-1 model.

Resumo

Nós calculamos, no contexto do modelo 3-3-1 com léptons pesados carregados, vínculos sobre alguns dos parâmetros das partículas extras do modelo ao impor que suas contribuições aos fatores $(g-2)$ do elétron e do múon estejam de acordo com os dados experimentais dentro de 1σ-3σ. Para obter resultados realistas nós consideramos algumas das possíveis soluções das matrizes unitárias esquerda e direita que diagonalizam as matrizes de massa leptônicas, dando as massas leptônicas observadas e ao mesmo tempo acomodando a matriz de mistura de Pontecorvo-Maki-Nakagawa-Sakata (PMNS). Nós mostramos que, ao menos até a ordem de 1-loop, na faixa de parâmetros explorada, não é possível acomodar simultaneamente os fatores $(g-2)$ do elétron e do múon a não ser que um dos léptons extras tenha massa da ordem de 20-40 GeVs e a escala de energia da simetria 331 esteja em torno de 60-80 TeVs.

Palavras chave: momento de dipolo magnético, múon, elétron, modelo 3-3-1.

Contents

List of Figures

1. Introduction

The electron and the muon have magnetic dipole moments (MDM), due to their spin. These MDMs interact with external magnetic fields, and in Quantum Mechanics these interactions are described by the following term in the Hamiltonian

$$H_\mu = -\vec{\mu} \cdot \vec{B} \qquad \vec{\mu} = g\frac{Qe}{2m}\vec{S}, \tag{1.1}$$

where e is the electron charge, Q is the electric charge of the particle (-1 for the electron and muon), m is the particle's mass and $\vec{S}$ is its spin. The factor g is known as the gyromagnetic factor. From Dirac's relativistic equation, Dirac himself found that $g = 2$, which agreed to the experimental results at the time. Later, with measurements of the hyperfine structure of hydrogen, is was found that $g \approx 2$. Part of such difference was first explained by Schiwnger, where he calculated the correction for the electron-photon vertex in QED (for more details see sec. 2.1). With such deviations of g with respect to 2, it is convenient to write

$$\vec{\mu} = 2(1+a)\frac{Qe}{2m}\vec{S} \qquad a = \frac{g-2}{2} \tag{1.2}$$

where the first term on the left (proportional to 2) is Dirac's prediction, and a embodies the corrections to the gyromagnetic factor. Such corrections are known as the anomalous magnetic dipole moment (AMDM).

Both anomalous magnetic dipole moments of electron and muon $a_{e,\mu} = (g-2)_{e,\mu}/2$, have been measured with great precision. We have $a_e^{\text{exp}} = 1.15965218076(28) \times 10^{-3}$ for the electron, and $a_\mu^{\text{exp}} = 1.1659209(6) \times 10^{-3}$ for the muon [1]. The theoretical calculations within the Standard Model (SM) have reached the high level of precision of the experiments. On one hand, the calculation for the electron a_e, considering only QED up to tenth order, gives the result of $a_e^{\text{SM}} = 1.159652181643(25)(23)(16)(763) \times 10^{-3}$ [2], giving a difference of

$$\Delta a_e = a_e^{\text{exp}} - a_e^{\text{SM}} = -0.91(82) \times 10^{-12}, \tag{1.3}$$

which is close to one standard deviation. On the other hand, for the muon a_μ, calculations considering QED up to five loops plus hadronic vacuum polarization up to next-to-leading order, hadronic light-by-light scattering and electroweak contributions, results in $a_\mu^{SM} = 1.16591801(49) \times 10^{-3}$ [3, 4, 5], leading to a difference between theory and experiment of

$$\Delta a_\mu = a_\mu^{\text{exp}} - a_\mu^{\text{SM}} = 2.87(80) \times 10^{-9}, \tag{1.4}$$

a difference that goes beyond three standard deviations from the experimental result.

This difference between the SM prediction and the experimental value of the muon anomalous magnetic moment has been studied in many models. For instance, in other 3-3-1 models [6, 8, 9, 10], left-right symmetric models [11], supersymmetric models [12, 13, 14, 15, 16] and two-Higgs doublets models [17, 18].

In particular, the 3-3-1 models are interesting extensions of the standard model (SM), since they solve some of the questions that the SM leaves without answer. For example, among others, the number of generations, why $\sin^2\theta_W < 1/4$, and electric charge quantization. The models have also interesting consequences in flavor physics [19, 20, 21] and, in particular, those 3-3-1 models with quarks with electric charge -4/3 and 5/3 (in units of $|e|$) have at least one neutral scalar which can appear as a heavy resonance that could be observed at LHC [22, 23, 24, 25]. The model has new singly and doubly charged vector bosons [26] and hadrons with electric charges $\pm(3, 4, 5)$ [27] that can also appear as LHC resonances. In fact, if the existence of these resonances is confirmed in the near future, one natural explanation for it is the minimal 3-3-1 model or the 3-3-1 model with heavy leptons. We use here *natural* in the sense that usually models are proposed just to solve particular discrepancies with the SM, as the latter ones. Meanwhile, 3-3-1 models assume a new set of gauge symmetries and explore their consequences, supposing that this new set of symmetries may explain all experimental results.

At the same time that the agreement between the experiment and the SM for the electron AMDM gives us confidence in the correctness of the theory, the disagreement in the muon case suggests that there may be effects unaccounted by the SM, or it is still possible that such effects come from new particles and through their interactions with the already known particles. For instance, the contributions of heavy leptons to the a_μ factor have been considered in gauge models since Refs. [28, 29]. However, we should not forget that for the AMDM of the muon to imply new physics, its value should disagree with the SM beyond 5σ.

In the literature, when the explanation of the observed value of the muon a_μ is based on new physics, its effects in the electron a_e are usually not taken into account, it is assumed that these effects do not perturb the values of the electron AMDM. Here we will show that, at least in this particular model, it is not possible to fit the Δa_e and Δa_μ with the same parameters considering 1-loop order calculations, unless one of the extra leptons has a mass of the order of 20-40 GeV and the energy scale of the 331 symmetry is of tens of TeVs. Also, usually in literature the charged lepton masses are neglected, thus allowing to obtain simple expressions for the Δa_μ. In the latter cases, $\Delta a_\mu(X) \propto m_\mu^2/M_X^2$, where M_X is the mass of some exotic particle. Although this case seems to be reasonable, we decided to not use such approximations, given the high precision of the experimental results. See chapter 8 for a more detailed discussion.

As a final remark, the work here presented has already been published. It can be found in [30], where a shorter version of what is discussed in this thesis is available.

2. The magnetic dipole moment in quantum field theory

Here we will briefly discuss how the magnetic dipole moment (MDM) of a particle is calculated, taking the correction to the electron-photon vertex as an example. Consider the diagram from Fig. 2.1 for an interaction between two electrons, where the circle on the left vertex is given by the corrections from the electron-photon vertex. This scattering amplitude is given by:

$$i\mathcal{M} = ie^2 \left[\bar{u}\left(p'\right)\Gamma^{\mu}\left(p,p'\right)u\left(p\right)\right]\frac{1}{q^2}\left[\bar{u}\left(k'\right)\gamma_{\mu}u\left(k\right)\right] \tag{2.1}$$

where Γ^{μ} represents the corrected vertex (a pictorial interpretation may be seen in Fig. 2.2). This term must transform as a vector (or pseudovector), therefore we can represent it as a linear combination of gamma matrices and momenta involved in the vertex [32]:

$$\Gamma^{\mu}\left(q\right) = F_1\left(q^2\right)\gamma^{\mu} + F_2\left(q^2\right)\frac{i\sigma^{\mu\nu}q_{\nu}}{2m} + F_A\left(q^2\right)\left(\gamma^{\mu}\gamma_5 q^2 - 2m\gamma_5 q^{\mu}\right) + F_3\left(q^2\right)\sigma^{\mu\nu}\gamma_5 q_{\nu} \tag{2.2}$$

where $q = p' - p$, m is the fermion mass and the F_x are the form factors. The terms proportional to F_A (axial current) and F_3 (electric dipole moment) do not contribute to the MDM. It is easy to see that because the MDM is CP invariant, while the terms proportional to F_A and F_3 are not, due to the γ_5 matrices.

Given that the MDM is an intrinsic propoerty of the particle, it must exist even

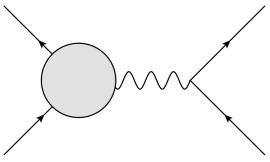

Figure 2.1.: Interaction of two electron mediated by a photon. The electrons are represented by continuous lines and the photon by the wavy line.

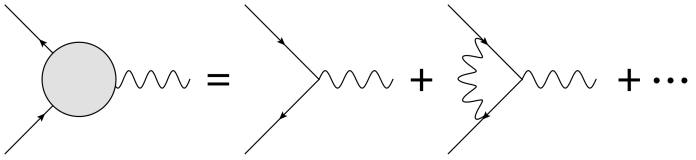

Figure 2.2.: The vertex in Fig. 2.1 can be understood as the sum of corrections coming from loops created by the interactions in a given theory.

when no interactions are present. Therefore, we consider the non-relativistic limit for its calculation. Also, it is possible to verify that the two first terms in Eq. 2.2, in the non-relativistic limit, reduce to the magnetic dipole moment operator from quantum mechanics. With just these two terms, our equation for the current becomes:

$$J^{\mu} = \bar{u}\left(p'\right)\left[F_1\left(q^2\right)\gamma^{\mu} + F_2\left(q^2\right)\frac{i\sigma^{\mu\nu}q_{\nu}}{2m}\right]u\left(p\right), \tag{2.3}$$

where we considered the first two terms from Eq. 2.2 to construct the electron-photon interaction current, because they are the only ones of interest to the MDM. Remebering that, for Dirac spinors in the non-relativistic limit, we can use the identity:

$$\Psi = \begin{pmatrix}\psi\\0\end{pmatrix} \tag{2.4}$$

where we are left with only the paticle spinor, being the antiparticle one negligible in the non-relativistic limit. With that, we have for the first term in the current

$$\begin{aligned}
\bar{u}\left(p'\right)\gamma^{i}u\left(p\right) &= \psi^{\dagger}\left[\left(p'_{j}\sigma^{j}\right)\sigma^{i} + \sigma^{i}\left(p_{j}\sigma^{j}\right)\right]\psi\\
&= \psi^{\dagger}\left[p'_{j}\left(\delta^{ji} + i\epsilon^{jik}\sigma^{k}\right) + p_{j}\left(\delta^{ij} + i\epsilon^{ijk}\sigma^{k}\right)\right]\psi\\
&= \psi^{\dagger}\left[\left(p'_{j} + p_{j}\right)\delta^{ij} + \left(p_{j} - p'_{j}\right)i\epsilon^{ijk}\sigma^{k}\right]\psi\\
&= \psi^{\dagger}\left[\left(p'_{i} + p_{i}\right) + i\epsilon^{ijk}q_{j}\sigma^{k}\right]\psi\\
&= \psi^{\dagger}\left[\left(p'_{i} + p_{i}\right) - i\epsilon^{ijk}q^{j}\sigma^{k}\right]\psi
\end{aligned} \tag{2.5}$$

and the second term

$$\begin{aligned}
\bar{u}\left(p'\right)\frac{i\sigma^{\mu\nu}q_{\nu}}{2m}u\left(p\right) &= 2m\psi^{\dagger}\left[\frac{i}{2m}\epsilon^{ijk}q_{j}\sigma^{k}\right]\psi\\
&= 2m\psi^{\dagger}\left[\frac{-i}{2m}\epsilon^{ijk}q^{j}\sigma^{k}\right]\psi,
\end{aligned} \tag{2.6}$$

where we used the Dirac representations for gamma matrices, simply substituting these in 2.3.

Considering only terms proportional to $\epsilon^{ijk}q^j\sigma^k$, we can write the following amplitude for the current interaction with the electromagnetic field $\vec{A}(q)$ as:

$$\begin{aligned} i\mathcal{M} &= -i\psi^\dagger\left[-i\epsilon^{ijk}q^j\sigma^k\left(F_1(0)+F_2(0)\right)\right]\psi A^i \\ &= i\psi\sigma^k\left[F_1(0)+F_2(0)\right]\psi B^k \end{aligned} \tag{2.7}$$

where $B^k(q) = -i\epsilon^{ijk}q^iA^j$ is the magnetic field as a momentum function (given by a Fourier transform). We considered $q^2 = 0$ because the MDM is independent of the momentum transfered between the fermion and the photon, once again due to the fact the the MDM is an instrinsic property of the particle. We can see that the amplitude represents a interaction between the fermionic spin ($\vec{\sigma}$) and the magnetic field ($\vec{B}$), which characterizes a contribution to the MDM.

Interpreting this amplitude in Born's approximation we can see that it corresponds to a potential with the form [33]:

$$V(x) = -\langle\vec{\mu}\rangle\cdot\vec{B}(x) \tag{2.8}$$

where

$$\langle\vec{\mu}\rangle = \frac{e}{m}\left[F_1(0)+F_2(0)\right]\psi^\dagger\frac{\vec{\sigma}}{2}\psi \tag{2.9}$$

This expression can be written in its more traditional form

$$\vec{\mu} = g\left(\frac{e}{2m}\right)\vec{S} \tag{2.10}$$

where $\vec{S}$ is the electron's spin. Comparing Eq. 1.2 and the above equations we see that

$$g = 2\left[F_1(0)+F_2(0)\right] = 2+2F_2(0)\,. \tag{2.11}$$

The factor $F_1(0)$ is equal to 1 in all perturbation orders, that is because of its relation with electrostatic interactions. Such factor gives us a measure of the electric charge perceived by a particle, this charge being equal to $F_1\left(q^2\right)\cdot e$, where e is the positron charge.

Meanwhile, the $F_2\left(q^2\right)$ factor, at first order in perturbation theory, is null. At higher orders it assumes a non-zero value, giving rise to a small difference of the MDM predicted by Dirac. These higher order contributions are the anomalous magnetic dipole moment (AMDM).

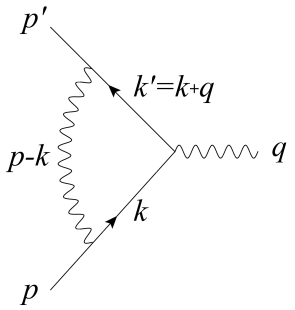

Figure 2.3.: Diagram for the electron-photon vertex first order correction. The momenta of each line are indicated in the figure.

2.1. First order correction for the electron-photon vertex

The first vertex correction comes from the photon creating a loop together with the fermion line. Starting from the diagram in Fig. 2.3 we find the following:

$$\begin{aligned}\delta\Gamma^{\mu} &= \int \frac{d^4k}{(2\pi)^4}\left[\frac{-ig_{\rho\nu}}{(k-p)^2+i\epsilon}\right](-ie\gamma^{\nu})\left[i\frac{\not{k}'+m}{k'^2-m^2+i\epsilon}\right]\gamma^{\mu}\left[i\frac{\not{k}+m}{k^2-m^2+i\epsilon}\right](-ie\gamma^{\rho}) \\ &= 2ie^2\int\frac{d^4k}{(2\pi)^4}\frac{\not{k}\gamma^{\mu}\not{k}'+m^2\gamma^{\mu}-2m\,(k+k')^{\mu}}{\left[(k-p)^2+i\epsilon\right]\left[k'^2-m^2+i\epsilon\right]\left[k^2-m^2+i\epsilon\right]}\end{aligned} \tag{2.12}$$

We can use Feynman's parametrization

$$\frac{1}{A_1\cdots A_n} = \int_0^1 dx_1\cdots dx_n\delta\left(x_1+\cdots+x_n-1\right)\frac{(n-1)!}{\left[x_1A_1+\cdots+x_nA_n\right]^n} \tag{2.13}$$

to write the denominator of our integral as:

$$\frac{1}{\left[(k-p)^2+i\epsilon\right]\left[k'^2-m^2+i\epsilon\right]\left[k^2-m^2+i\epsilon\right]} = \int_0^1 dxdydz\delta\left(x+y+z-1\right)\frac{2}{D^3} \tag{2.14}$$

where we have

$$\begin{aligned}D &= x\left[k^2-m^2+i\epsilon\right]+y\left[k'^2-m^2+i\epsilon\right]+z\left[(k-p)^2+i\epsilon\right] \\ &= x\left(k^2-m^2\right)+y\left(k^2+q^2+2k\cdot q-m^2\right)+z\left(k^2+p^2-2k\cdot p\right)+(x+y+z)\,i\epsilon \\ &= k^2+2yk\cdot q-2zk\cdot p-xm^2+y\left(q^2-m^2\right)+zp^2+i\epsilon\end{aligned} \tag{2.15}$$

where, in the above equations, we used the identity $x+y+z=1$. Defining $l=k+yq-zp$, we can write

$$D=l^2-\left(-2yzq\cdot p+y^2q^2+z^2p^2\right)-xm^2+y\left(q^2-m^2\right)+zp^2+i\epsilon \tag{2.16}$$

Knowing that:

$$p\cdot q=p\cdot\left(p'-p\right)=p\cdot p'-m^2 \tag{2.17}$$

$$q^2=\left(p'-p\right)^2=2m^2-2p\cdot p' \tag{2.18}$$

we have

$$p\cdot q=-\frac{q^2}{2} \tag{2.19}$$

Which allows us to write the denominator as

$$\begin{aligned} D&=l^2+2yz\left(-q^2/2\right)-y^2q^2+y\left(q^2-m^2\right)-z^2m^2+zm^2-xm^2+i\epsilon\\ &=l^2+q^2xy-m^2\left(1-z\right)^2+i\epsilon \end{aligned} \tag{2.20}$$

Now we can write again the vertex

$$\delta\Gamma^\mu=2ie^2\int\frac{d^4k}{\left(2\pi\right)^4}dxdydz\delta(x+y+z-1)\frac{2\left[\not{k}\gamma^\mu\not{k}'+m^2\gamma^\mu-2m\left(k+k'\right)^\mu\right]}{\left[l^2+q^2xy-m^2\left(1-z\right)^2+i\epsilon\right]^3} \tag{2.21}$$

Moving on, now we worry about the integral's numerator, first writing it as a function of l:

$$\begin{aligned} N^\mu&=\not{k}\gamma^\mu\not{k}'+m^2\gamma^\mu-2m\left(k+k'\right)^\mu\\ &=\left(\not{l}-y\not{q}+z\not{p}\right)\gamma^\mu\left(\not{l}+\not{q}\left(1-y\right)+z\not{p}\right)-2m\left(2l+q\left(1-2y\right)+2zp\right)^\mu \end{aligned} \tag{2.22}$$

and with the identities

$$\int\frac{d^4l}{\left(2\pi\right)^4}\frac{l^\mu}{D^3}=0 \tag{2.23}$$

$$\int\frac{d^4l}{\left(2\pi\right)^4}\frac{l^\mu l^\nu}{D^3}=\int\frac{d^4l}{\left(2\pi\right)^4}\frac{\frac{1}{4}g^{\mu\nu}l^2}{D^3} \tag{2.24}$$

the numerator becomes

$$\begin{aligned} N^\mu=&-\frac{l^2}{2}\gamma^\mu+\left(-y\not{q}+z\not{p}\right)\gamma^\mu\left(\not{q}\left(1-y\right)+z\not{p}\right)+m^2\gamma^\mu\\ &-2m\left(q\left(1-2y\right)+2zp\right)^\mu\\ =&-\frac{l^2}{2}\gamma^\mu+y\left(1-y+z\right)\not{p}'\gamma^\mu\not{p}+\left(z-y\right)\left(1-y+z\right)\left[2p^\mu\not{p}-m^2\gamma^\mu\right]\\ &-y\left(y-1\right)\left[2p'^\mu\not{p}'-m^2\gamma^\mu\right]-2m\left[q\left(1-2y\right)+2zp\right]^\mu+m^2\gamma^\mu\\ &-\left(z-y\right)\left(1-y\right)\left\{2\left[p'^\mu\not{p}+\left(m^2-q^2/2\right)\gamma^\mu-p^\mu\not{p}'\right]+\not{p}'\gamma^\mu\not{p}\right\} \end{aligned} \tag{2.25}$$

To obtain $\bar{u}(p')N^{\mu}u(p)$, we can use the identities $\bar{u}(p')\not{p}' = m\bar{u}(p')$ and $\not{p}u(p) = mu(p)$ in the numerator, such that:

$$\begin{aligned} N^{\mu} =& \gamma^{\mu}\left[-\frac{l^2}{2} + (1-x)(1-y)q^2 + \left(1-2z+z^2\right)m^2\right] \\ &+ \left(p'^{\mu}+p^{\mu}\right)mz(z-1) + q^{\mu}m(z-2)(x-y) \end{aligned} \tag{2.26}$$

Using Ward's identity for QED, $q_{\mu}\Gamma^{\mu} = 0$, we see that we can neglect the term linear in q^{μ}. Now, using Gordon's identity

$$\bar{u}(p')\gamma^{\mu}u(p) = \bar{u}(p')\left[\frac{p'^{\mu}+p^{\mu}}{2m} + \frac{i\sigma^{\mu\nu}q_{\nu}}{2m}\right]u(p) \tag{2.27}$$

we can replace the term proportional to $p'^{\mu}+p^{\mu}$ and write

$$\begin{aligned} \bar{u}(p')\delta\Gamma^{\mu}u(p) =& 2ie^2\int\frac{d^4l}{(2\pi)^4}\int_0^1 dxdydz\delta(x+y+z-1)\frac{2}{D^3} \\ &\times\bar{u}(p')\left\{\gamma^{\mu}\left[-\frac{l^2}{2} + (1-x)(1-y)q^2 + \left(1-4z+z^2\right)m^2\right]\right. \\ &\left.+\frac{i\sigma^{\mu\nu}q_{\nu}}{2m}\left[2m^2z(1-z)\right]\right\}u(p) \end{aligned} \tag{2.28}$$

Comparing Eq. 2.28 with Eq. 2.3 we can identify the form factors $F_1\left(q^2\right)$ and $F_2\left(q^2\right)$ with the terms that multiply γ^{μ} and $i\sigma^{\mu\nu}q_{\nu}/2m$, respectively. To find $F_2\left(q^2\right)$ we shall use the identity

$$\int\frac{d^4l}{(2\pi)^4}\frac{1}{\left(l^2-\Delta\right)^m} = \frac{i(-1)^m}{(4\pi)^2}\frac{1}{(m-1)(m-2)}\frac{1}{\Delta^{m-2}} \tag{2.29}$$

such that

$$F_2\left(q^2\right) = \frac{\alpha}{2\pi}\int_0^1 dxdydz\delta(x+y+z-1)\frac{2m^2z(1-z)}{-xyq^2+(1-z)^2m^2} \tag{2.30}$$

The MDM contribution is given by the form factor evaluated at $q^2 = 0$, according to 2.11. In this manner, at our case of interest

$$\begin{aligned} F_2(0) &= \frac{\alpha}{2\pi}\int_0^1 dxdydz\delta(x+y+z-1)\frac{2z}{1-z} \\ &= \frac{\alpha}{2\pi} \approx 0,0011614 \end{aligned} \tag{2.31}$$

where we finally find the first order contribution for the electron's anomalous MDM. Comparing with the experimental values given by [1], where $F_2(0) = 0,0011597$, we see

that the first order prediction has a 0.02% difference with respect to the experimental results, not bad for a first order calculation.

This example, for the 1-loop photon contribution to the electron AMDM, can be extended to contributions from other processes and from other models. To find these contributions, it is necessary to calculate all Feynman diagrams that correct the fermion-photon vertex, then all the amplitudes are summed and the coefficient multiplying the term $i\sigma_{\mu\nu}q_\nu/2m$ (i.e. the second term in Eq. 2.3), identified as $F_2(q)$, has to be evaluated at null momentum ($q = 0$). This $F_2(0)$ is the contribution to the anomalous magnetic moment. This is the procedure we will follow in this work to calculate the contributions of the 3-3-1 model with heavy leptons (331HL) to the muon and electron AMDMs, and it is also the procedure followed to calculate the SM contributions, which we shall discuss in the next chapter.

3. Standard Model prediction for the muon AMDM

Many of the SM contributions for the muon AMDM have been calculated throughout several works (see [4] and references therein), up to 5-loop diagrams. Given the diversity of results, we will separate them in three categories: Pure quantum electrodynamics (QED), hadronic contributions in QED, and electroweak contributions.

3.1. Pure quantum electrodynamics

These contributions are the dominating ones, having been calculated up to 5-loops. These diagrams involve only leptons and photons and they can be divided in two categories: diagrams where the external and internal leptons are all of the same flavor, and diagrams where some or all the internal leptons are different from the external ones.

In the first case, diagrams from 1 up to 3 loops were all calculated analytically, 4-loops have some numerical and some analytical results, and 5-loops have only numerical results. In the second case, 2 and 3 loop results are all analytical and 4-loop results are analytical and numerical. The total contribution coming from these two cases to the muon MDM is $a_\mu^{QED} = 116584718.09(0.15) \times 10^{-11}$.

3.2. Hadronic contributions in QED

Besides leptons in the internal lines of a diagram, hadrons can be present as well, giving their own contributions. These electromagnetic interactions between hadrons produces contributions induced by hadronic vacuum polarization (HVP) and hadronic light-by-light scattering (HLbyL).

HVP contributions come from vacuum corrections to the photon propagator, represented by the circle in Fig. 3.2. Such corrections are based on the spectral representation,

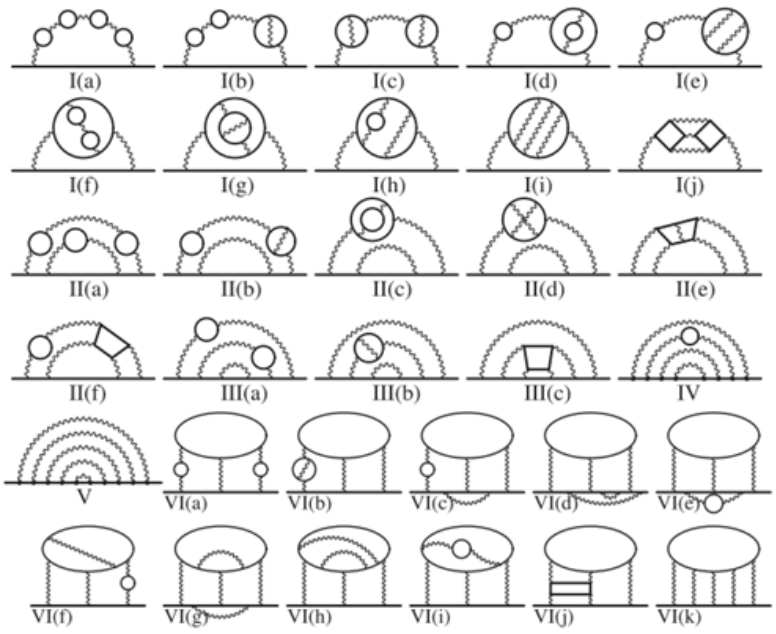

Figure 3.1.: Examples of QED diagrams contributing to the muon MDM. These are 10th order examples of diagrams that contribute to the muon MDM. The solid lines represent leptons and the wavy lines photons.

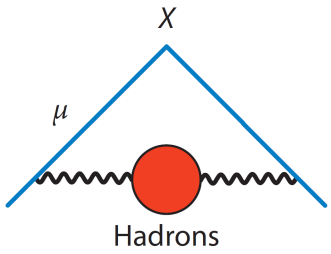

Figure 3.2.: Hadronic vacuum polarization contribution to the MDM. The red circle represents the corrections to the photon propagator while the X is where the external photon is connected to the diagram.

where the full propagator is given by a linear combination of all the free propagators in the theory, and the coefficients for this linear combination are given by experimental data. In leading order calculations, the HVP contribution is $a_\mu^{HVP-LO} = 6923(42) \times 10^{-11}$ and next-to-leading order is $a_\mu^{HVP-NLO} = 98.4(0.7) \times 10^{-11}$.

Hadronic light-by-light scattering comes from an effective 4-photon vertex, as shown in Fig. 3.3. Contrary to the HVP case, the HLbyL case has no experimental input available (photon-photon scattering data) for its calculation, therefore relying solely on theoretical results. So far, the most rigorous result come from large-N_c limits (where it is assumed that the number of colors in the chromodynamic sector is very large), giving a contribution of $a_\mu^{HLbyL} = 105(26) \times 10^{11}$ to the muon MDM. It is expected that lattice QCD techniques may provide better first-principles estimates in the future.

3.3. Electroweak contributions

This class of contributions considers diagrams involving only particles from the electroweak sector of the SM (i.e. fermions, gauge bosons and the Higgs boson). Examples of these diagrams can be seen in Fig. 3.4. There are results for 1 and 2 loops, being the 1-loop results all analytical. The 2-loop cases are subdivided in two categories, when there is a closed fermion loop and when there are bosonic corrections. In the latter case the results are obtained using an expansion in powers of $sin^2\theta_W$, where terms proportional to $log(M_W^2/m_\mu^2)$, $log(M_H^2/m_W^2)$, $(M_W^2/M_H^2)log(M_H^2/m_W^2)$, M_W^2/M_H^2 and constant terms are kept. In the fermion-loop case, when the fermions are heavy, the approximation $m_f/m_\mu >> 1$ is used, when the fermion is light effective theories are considered. In total, these two types of diagrams contribute to the muon MDM as $a_\mu^{EW} = 153(1) \times 10^{-11}$.

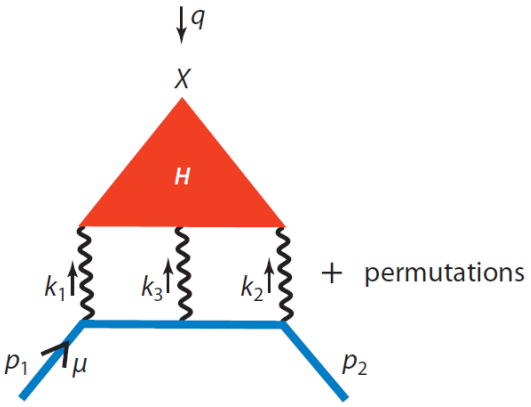

Figure 3.3.: Hadronic light-by-light scattering contribution to the MDM. The red triangle represents the effective 4-photon vertex while the X is where the external photon is connected to the diagram.

3.4. Total Standard Model contribution

Considering all contributions discussed in the sections above, their total contribution to the muon anomalous magnetic dipole moment is $a_\mu^{SM} = 1.16591801(49) \times 10^{-3}$. If we compare this with the experimental result of $a_\mu^{\text{exp}} = 1.1659209(6) \times 10^{-3}$, the difference is

$$\Delta a_\mu = a_\mu^{\text{exp}} - a_\mu^{\text{SM}} = 2.87(80) \times 10^{-9}, \tag{3.1}$$

a difference that goes beyond three standard deviations from the experimental result.

This difference may become smaller with further calculations, either by exploring diagrams up to higher orders or by improving the ones done for the already explored diagrams. However, it is possible that even with such improvements this difference

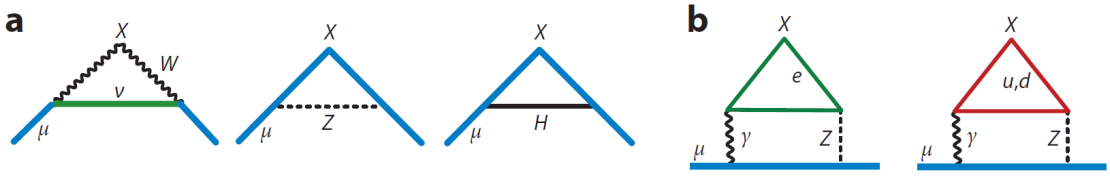

Figure 3.4.: Electroweak contributions to the MDM. (a) 1-loop level contributions, where X indicates the vertex connecting to the photon. (b) Two-loop electroweak diagrams generated by the $\gamma\gamma Z$ triangle for the first family.

Contribution	Result (10^{-11})
QED	116 584 718.09 (0.15)
HVP-LO	6923(42)
HVP-NLO	-98.4 (0.7)
EW	153(1)
Total	116592090(6)

Table 3.1.: Standard Model contributions to the muon AMDM.

persists, and this leaves room for explorations of new alternatives to the SM, such as the 3-3-1 model with heavy leptons, which we shall present in the following chapters.

4. The 3-3-1 model

Models with gauge symmetry $SU(3)_C \otimes SU(3)_L \otimes U(1)_X$ present new possibilities for the electroweak interactions, thanks to the $SU(3)_L$ symmetry, different from the $SU(2)_L$ used in the SM. Here we consider the 3-3-1 model with heavy charged leptons (331HL for short) in which there are new exotic quarks and leptons. Moreover, to give mass to all the particles, more scalar fields are needed. Hence, these models are intrinsically multi-Higgs models. In this model the electric charge operator is given by $Q/|e| = T_3 - \sqrt{3}T_8 + X$ [31], where e is the electron charge, $T_{3,8} = \lambda_{3,8}/2$ (being $\lambda_{3,8}$ the Gell-Mann matrices) and X is the hypercharge operator associated to the $U(1)_X$ group [1]. In the sections below we will present the particle content of the model, with its charges associated to each group in the parentheses, in the form $(SU(3)_C,\ SU(3)_L,\ U(1)_X)$.

4.1. Leptons

The substitution of the $SU(2)_L$ symmetry for a $SU(3)_L$ one (comparing with the Standard Model), means that now the fermions are grouped into triplets. However, the third component differs from one 3-3-1 model to another. In the case of the 331HL, the third component is an exotic, positively charged, heavy lepton. In some models, the third component is a positron, in others a neutrino or even an exotic neutral heavy particle. For the 3-3-1 model with heavy leptons, the leptonic sector has a left handed triplet and two right handed singlets, defined as follows:

$$\Psi_{aL} = \begin{pmatrix} \nu_a \\ l_a^- \\ E_a^+ \end{pmatrix} \sim (1, 3, 0) \tag{4.1}$$

$$l_{aR}^- \sim (1, 1, -1) \qquad E_{aR}^+ \sim (1, 1, 1) \tag{4.2}$$

[1] Other 3-3-1 models may have different charge operators, where the constant multiplying T_8 can be $\pm\sqrt{3}$ or $\pm 1/\sqrt{3}$. This leads to a distinct particle content in all sectors.

where indices L and R indicate left and right handed spinors, respectively, and $a = e, \mu, \tau$.

4.2. Quarks

Even tough we won't need the quarks for the calculations of the AMDM's, we will present this sector. Here, there are two anti-triplets and one triplet, both left handed; besides the right handed singlets.

$$Q_{mL} = \begin{pmatrix} d_m \\ -u_m \\ j_m \end{pmatrix} \sim (3, 3^*, -1/3)\,, \qquad Q_{3L} = \begin{pmatrix} u_3 \\ d_3 \\ J \end{pmatrix} \sim (3, 3, 2/3) \tag{4.3}$$

$$u_{\alpha R} \sim (3, 1, 2/3)\,, \quad d_{\alpha R} \sim (3, 1, -1/3)\,, \quad j_{mR} \sim (3, 1, -4/3)\,, \quad J_R \sim (3, 1, 5/3) \tag{4.4}$$

where $m = 1, 2$ e $\alpha = 1, 2, 3$. The exotic quarks $j_{1,2}$ and J have electric charges -4/3 and 5/3, respectively.

4.3. Scalars

The scalar sector for the 331HL is formed by three triplets:

$$\chi' = \begin{pmatrix} \chi'^{-} \\ \chi'^{--} \\ \chi'^{0} \end{pmatrix} \sim (1, 3, -1)\,, \qquad \rho' = \begin{pmatrix} \rho'^{+} \\ \rho'^{0} \\ \rho'^{++} \end{pmatrix} \sim (1, 3, 1)\,, \qquad \eta' = \begin{pmatrix} \eta'^{0} \\ \eta_1'^{-} \\ \eta_2'^{+} \end{pmatrix} \sim (1, 3, 0) \tag{4.5}$$

where $\psi^0 = \frac{v_\psi}{\sqrt{2}}\left(1 + \frac{X_\psi^0 + iI_\psi^0}{|v_\psi|}\right)$ and $v_\psi = |v_\psi| e^{i\theta_\psi}$, for $\psi = \chi$, η, ρ. Given that the model has a $SU(3)$ symmetry in its scalar sector we can do the following transformation

$$U = \begin{pmatrix} e^{-i\theta_\eta} & 0 & 0 \\ 0 & e^{-i\theta_\rho} & 0 \\ 0 & 0 & e^{i(\theta_\eta + \theta_\rho)} \end{pmatrix} \tag{4.6}$$

With this the triplets become

$$\chi = \begin{pmatrix} \chi^{-} \\ \chi^{--} \\ \chi^{0} \end{pmatrix} \sim (0, 3, -1)\,, \qquad \rho = \begin{pmatrix} \rho^{+} \\ \rho^{0} \\ \rho^{++} \end{pmatrix} \sim (0, 3, 1)\,, \qquad \eta = \begin{pmatrix} \eta^{0} \\ \eta_1^{-} \\ \eta_2^{+} \end{pmatrix} \sim (0, 3, 0) \tag{4.7}$$

Now only the χ triplet has a complex phase in its vacuum expectation value, which means, $v_\rho = |v_\rho|$, $v_\eta = |v_\eta|$ and $v_\chi = |v_\chi| e^{i(\theta'_\eta + \theta'_\rho + \theta'_\chi)} = |v_\chi| e^{i\theta_\chi}$. With this, θ_χ becomes a new source of CP violation, in addition to the CKM and PMNS matrices already present in the SM. Also, some of the matrices that diagonalize the fermion mass matrices may appear in the interaction vertices, not just as the products that generate the CKM and PMNS matrices, but in other combinations as well (see appendix C.1). Given that the MDM is not related to CP violation, we will not consider its effects throughout this work.

The most general scalar potential is given by

$$\begin{aligned} V(\chi,\eta,\rho) &= \mu_1^2 \chi^\dagger\chi + \mu_2^2 \eta^\dagger\eta + \mu_3^2 \rho^\dagger\rho + (\alpha\, \epsilon_{ijk}\chi_i\rho_j\eta_k + H.c.) + a_1\left(\chi^\dagger\chi\right)^2 \\ &+ a_2\left(\eta^\dagger\eta\right)^2 + a_3\left(\rho^\dagger\rho\right)^2 + a_4\left(\chi^\dagger\chi\right)\left(\eta^\dagger\eta\right) + a_5\left(\chi^\dagger\chi\right)\left(\rho^\dagger\rho\right) \\ &+ a_6\left(\rho^\dagger\rho\right)\left(\eta^\dagger\eta\right) + a_7\left(\chi^\dagger\eta\right)\left(\eta^\dagger\chi\right) + a_8\left(\chi^\dagger\rho\right)\left(\rho^\dagger\chi\right) \\ &+ a_9\left(\rho^\dagger\eta\right)\left(\eta^\dagger\rho\right) + a_{10}[(\chi^\dagger\eta)(\rho^\dagger\eta) + (\eta^\dagger\chi)(\eta^\dagger\rho)] \end{aligned} \tag{4.8}$$

where we assume all coupling constants to be real[2]. The scalar potential with $a_{10} = 0$ has been considered for instance in Ref. [41, 34]. If this term is not zero, comparing with the aforementioned references, the only sector which is modified is that of the singly charged scalars.

This model is taken to the SM through the spontaneous symmetry breaking from the Higgs mechanism, in the following sequence: $SU(3)_L \otimes U(1)_X \to SU(2)_L \otimes U(1)_Y \to U(1)_{EM}$. The first break will make 4 out of the 9 generators of the group $SU(3)_L \otimes U(1)_X$ preserve the symmetry of the first vacuum, taking us to the $SU(2)_L \otimes U(1)_Y$ group from the SM. In the second break there will be only one generator left unbroken, the $U(1)_{EM}$ from electromagnetism. The passage from 331HL to SM is thanks to the symmetry break caused by the χ triplet, the second one, which takes us to the electromagnetism group, can happen either through the η or the ρ triplet.

From the potential above we calculate the mass eigenstates for the scalars, which will be important in finding all the necessary vertices for our calculations. The mass matrices and eigenstates are presented in the appendix B.

[2]In the most general case the coupling constants would be complex.

4.4. Yukawa interactions

The Yukawa Lagrangian in the leptonic sector is given by:

$$-\mathcal{L}_Y^l = G_{ab}^{\nu}\bar{\Psi}_{aL}\nu'_{bR}\eta + G_{ab}^{l}\bar{\Psi}_{aL}l'^{-}_{bR}\rho + G_{ab}^{E}\bar{\Psi}_{aL}E'^{+}_{bR}\chi + H.C. \tag{4.9}$$

where G^{ν}, G^{l} and G^{E} are arbitrary 3×3 matrices. From (4.9), we obtain the Yukawa interactions given in Appendix C and the mass matrices for the leptons, which are given by $M^l = G^l|v_\rho|/\sqrt{2}$ for the l'-type leptons and $M^E = G^E|v_\chi|e^{i\theta_\chi}/\sqrt{2}$ for the E'-type leptons. For simplicity we are assuming the G^E matrix to be diagonal. In this manner, for our masses to be real, we need the elements of the G^E matrix to have the form $(G^E)_{ii} = |G^E|_{ii}e^{-i\theta_\chi}$, which implies $m_{E_i} = G^E_{ii}|v_\chi|/\sqrt{2}$ (where $E_1 = E_e, E_2 = E_\mu, E_3 = E_\tau$). Notice from Eq. (4.9) that in the 331HL model there are no flavor changing neutral currents mediated by scalar fields. Moreover, we note that the interaction $\bar{E}'_{aL}\nu'_{bR}\eta_2^+$ does exist and, as we will show later, it is important to make the extra leptons E' unstable.

The mass eigenstates for the non-exotic leptons are obtained as $l'_{L,R} = (V^l_{L,R})^\dagger l_{L,R}$, where $l' = (l_1, l_2, l_3)$, and $l = (e, \mu, \tau)$ (the neutrinos symmetry eigenstates corresponds to the mass eigenstates, since we are assuming them to be massless). These $V^l_{L,R}$ matrices diagonalize the mass matrix in the following manner: $V^l_L M^l V^{l\dagger}_R = diag(m_e, m_\mu, m_\tau)$. Possible solutions for the $V^l_{L,R}$ matrices and the G^l matrix can be found in [34] and [37]. To find these solutions it was considered $|v_\rho| = 54$ GeV and $|v_\eta| = 240$ GeV, as in Ref. [35], these will be used in our analysis of the muon and electron AMDMs. Since the masses of the exotic leptons are unknown, we cannot find such solution for them, and for this reason, we considered their mass matrix diagonal to simplfy our calculations.

Although neutrinos get mass, say by the type-I seesaw mechanism [38], because of the small neutrino masses, the effect of unitary matrices in the vertices involving singly charged scalars, for all practical processes, is negligible in its non-diagonal elements: they are suppressed by the small neutrino masses. The neutrino masses are not of direct interest for the calculation of the AMDM, which we will assume massless here. We only note that if V^ν_L, is the matrix that diagonalizes the active neutrino masses, we can define the PMNS matrix as $V_{PMNS} = V^{l\dagger}_L V^\nu_L$. Then, it is possible to accommodate both PMNS and the active neutrino masses as it was done in Refs. [38, 37].

4.5. Gauge fields

Using the conventions presented in [7], the covariant derivatives involving the gauge fields are

$$\begin{aligned} D_\mu\phi &= \left(\partial_\mu - igW_\mu^a T_a - ig_x X B_\mu\right)\phi, \\ D_\mu\Psi_R &= \left(\partial_\mu - ig_x X B_\mu\right)\Psi_R, \\ D_\mu\Psi_L &= \left(\partial_\mu - igW_\mu^a T_a - ig_x X B_\mu\right)\Psi_L, \end{aligned} \tag{4.10}$$

where ϕ denotes a scalar, Ψ_L a left handed spinor, Ψ_R a right handed spinor, $T^a = \lambda^a/2$ - where λ^a are the Gell-Mann matrices - and X is the charge operator associated to the $U(1)_X$ group.

The mass eigenstates for the gauge bosons are obtained by acting the covariant derivatives on the scalar triplets. This derivative becomes clearer if we write

$$\mathcal{M}_\mu = \begin{pmatrix} W_\mu^3 + \frac{1}{\sqrt{3}}W_\mu^8 + 2tXB_\mu & \sqrt{2}W_\mu^+ & \sqrt{2}V_\mu^- \\ \sqrt{2}W_\mu^- & -W_\mu^3 + \frac{1}{\sqrt{3}}W_\mu^8 + 2tXB_\mu & \sqrt{2}U_\mu^{--} \\ \sqrt{2}V_\mu^+ & \sqrt{2}U_\mu^{++} & -\frac{2}{\sqrt{3}}W_\mu^8 + 2tXB_\mu \end{pmatrix}, \tag{4.11}$$

where $\mathcal{M}_\mu = W_\mu^a\lambda_a + 2tXB_\mu$ and $t = g_x/g$. With these identities the covariant derivatives can be written as

$$\begin{aligned} D_\mu\phi &= \partial_\mu\phi - i\tfrac{g}{2}\mathcal{M}_\mu\phi, \\ D_\mu\Psi_R &= \left(\partial_\mu - ig_x X B_\mu\right)\Psi_R, \\ D_\mu\Psi_L &= \left(\partial_\mu - i\tfrac{g}{2}\mathcal{M}_\mu\right)\Psi_L. \end{aligned} \tag{4.12}$$

The non-Hermitian gauge bosons are defined as

$$\begin{aligned} W_\mu^\pm &= \left(W_\mu^1 \mp iW_\mu^2\right)/\sqrt{2}, \\ V_\mu^\pm &= \left(W_\mu^4 \pm iW_\mu^5\right)/\sqrt{2}, \\ U_\mu^{\pm\pm} &= \left(W_\mu^6 \pm iW_\mu^7\right)/\sqrt{2}, \end{aligned} \tag{4.13}$$

with masses

$$\begin{aligned} m_W^2 &= \tfrac{1}{4}g^2v_W^2, \\ m_V^2 &= \tfrac{1}{4}g^2\left(|v_\eta|^2 + |v_\chi|^2\right), \\ m_U^2 &= \tfrac{1}{4}g^2\left(|v_\rho|^2 + |v_\chi|^2\right), \end{aligned} \tag{4.14}$$

where $v_W^2 = |v_\eta|^2 + |v_\rho|^2$.

Meanwhile, the neutral mass eigensatates can be written as a combination of the symmetry eigenstates

$$A^\mu = s_W W_3^\mu - \sqrt{3} s_W W_8^\mu + \sqrt{1-4s_W^2} B^\mu, \tag{4.15}$$

$$Z^\mu = -c_W W_3^\mu - \sqrt{3} s_W t_W W_8^\mu + t_W \sqrt{1-4s_W^2} B^\mu, \tag{4.16}$$

$$Z'^\mu = \frac{\sqrt{1-4s_W^2}}{c_W} W_8^\mu + \sqrt{3} t_W B^\mu, \tag{4.17}$$

where c_W, s_W and t_W are the cosine, sine and tangent of the Weinberg angle, respectively. They are related to the gauge constants as

$$t = \frac{g_x}{g} = \frac{s_W}{\sqrt{1-4s_W^2}}. \tag{4.18}$$

The neutral gauge bosons have the following masses

$$m_A^2 = 0 \tag{4.19}$$

$$m_Z^2 = = \frac{g^2}{4c_W^2}\left(v_\eta^2 + v_\rho^2\right) \tag{4.20}$$

$$M_{Z'}^2 = g^2 v_\chi^2 \left[\frac{s_W^4 \left(4 - \frac{\left(v_\eta^2+v_\rho^2\right)^2}{v_\chi^4}\right) + \left(1-2s_W^2\right)\left(\frac{v_\eta^2+v_\rho^2}{v_\chi^2}+4\right)}{12c_W^2\left(1-4s_W^2\right)} \right] \tag{4.21}$$

5. MDM in the 331HL model

In the 331HL model, the main extra contributions to MDMs arise from the heavy leptons, several scalars and vector bileptons (see Fig. 5.1). Here we present the one-loop contributions due to these particles in the model. We consider the scalar-lepton vertices to have the form $i(S_\xi + P_\xi\gamma_5)$ where $\xi = h_i, A^0, Y_1^+, Y^{++}$, with the factors S_ξ, P_ξ given in Eqs. (C.2)-(C.4). The vector-lepton vertices are considered to have the form $i\gamma^\mu(V_U - A_U\gamma_5)$ for the vector U^{--} and $i\gamma^\mu(f_V - f_A\gamma_5)$ for the vector Z'. All these couplings are given in Eqs. (C.10)-(C.14). We present the general result below, valid either for the electron or the muon (the diagrams were calculated in the unitary gauge). The full result comes from considering all the possible one-loop diagrams involving any exotic lepton, scalar or vector particles.

We will verify if the extra contributions in the 331HL model are enough to satisfy the constraints in Eqs. (1.3) and (1.4). In this case, all considered diagrams are those shown in Fig. 5.1. The muon MDM has been considered in the context of other 3-3-1 models in [6, 8, 9], however, there the authors did not consider the lepton mixing and also the constraints coming from the electron $(g-2)_e$. As can be seen in the matrices shown in Secs. 6.1.2-6.1.5, it is possible that there are important non-diagonal entries in the matrix V_L^l. Moreover, solving the muon Δa_μ discrepancy and at the same time giving contributions compatible with Δa_e is not a trivial issue, at least in 1-loop order.

As said before, we consider only the extra diagrams present in the model as being responsible for the new contributions to the Δa_μ, such that

$$a_i^{331} = \Delta a_i = a_i^{exp} - a_i^{SM}, \quad i = e, \mu, \tag{5.1}$$

where a_i^{331} includes diagrams with at least one of the extra particles in the model, i.e., only contributions coming from beyond SM physics. These are shown in Fig. 5.1.

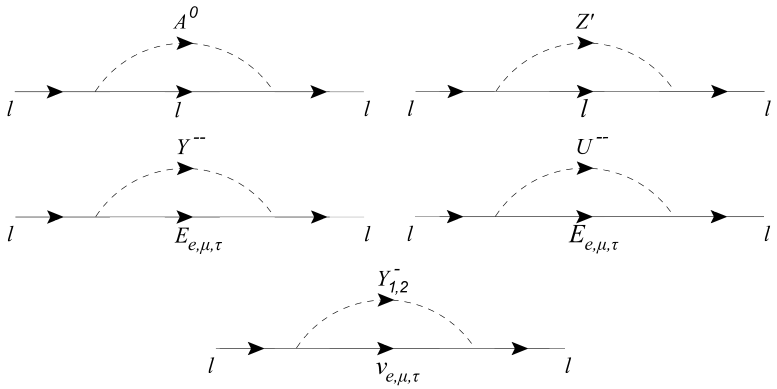

Figure 5.1.: One loop diagrams for the MDM. The fermion l indicates either an electron or a muon. The 3-3-1 model contribution to the MDM comes from all these diagrams, considering two cases, when the photon is connected to the fermion and when the photon is connected to the boson (when applicable).

5.1. Scalar contributions

Unlike the minimal 331 model, in the present one there are no flavor changing neutral currents (FCNC) through the Higgs exchange. In this situation a neutral scalar S has only scalar interactions $\bar{f}fS$, and a pseudo-scalar A has only pseudo-scalar interactions $\bar{f}\gamma_5 fA$. We will denote the respective factors S^l_ξ and P^l_ξ where l denotes the external lepton and ξ denotes the scalar in the loop.

First, we consider the case in which there is a neutral or charged scalar, denoted by ξ, in the loop. When the photon is connected to the fermion line, corresponding to diagram a in Fig. 5.2, we have:

$$\Delta a^l_\xi(f) = -\frac{Q_I}{96\pi^2} m_l^2 \frac{1}{M_\xi^2} \int_0^1 dx \frac{|P^l_\xi|^2 F^\xi_P(x,\epsilon^\xi_l) + |S^l_\xi|^2 F^\xi_S(x,\epsilon^\xi_l)}{F^\xi(x,\epsilon^\xi_l,\lambda^\xi_l)}, \tag{5.2}$$

with $\epsilon^\xi_l = m_I/m_l$, $\lambda^\xi_l = m_l/M_\xi$, and $\xi = h_1, A, Y^-_1, Y^{--}$, m_l is the mass of the electron or muon, m_I is the mass of the fermion in the loop, and M_ξ is the scalar mass in the loop; S^l_ξ and P^l_ξ are the matrices given in Eq. (C.2) and depend on the type of the scalar, Q_I is the electric charge of the internal lepton. We have defined

$$\begin{aligned}
F^\xi_S(x,\epsilon^\xi_l) &= -g(x) + 12\epsilon^\xi_l(x+1),\\
F^\xi_P(x,\epsilon^\xi_l) &= g(x) + 12\epsilon^\xi_l(x+1),\\
F^\xi(x,\epsilon^\xi_l,\lambda^\xi_l) &= x[(\lambda^\xi_l)^2(x-1)+1] - (\epsilon^\xi_l\lambda^\xi_l)^2(x-1),
\end{aligned} \tag{5.3}$$

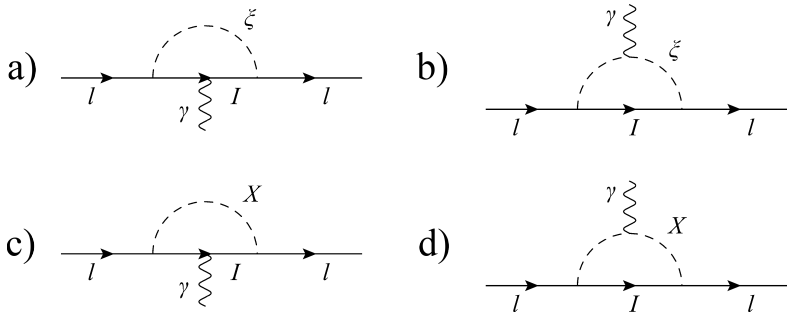

Figure 5.2.: Types of one loop diagrams for the MDM. The fermion l indicates either an electron or a muon, I is a fermion internal to the loop, X denotes a gauge boson, ξ denotes a scalar and γ denotes a photon. In diagram a) we have the case where there is a scalar in the loop and the photon is connected to the internal fermion (Eq. 5.2), while in b) the photon is connected to the scalar (Eq. 5.4). In diagram c) we have a vector gauge boson in the loop with the photon connected to the fermion (Eq. 5.9) and in d) the photon is connected to the gauge boson (Eq. 5.7).

and $\epsilon_l^{h,A} = 1$ (again, this is because there are no flavor changing neutral currents via neutral scalar or pseudo-scalars) and $\epsilon_l^{Y^{--}} = m_I/m_l$, with $M_I = E_e, E_\mu, E_\tau$, and $\epsilon_l^{Y_1^-} = m_\nu/m_l$; we have also defined $g(x) = 12x^2 + 9x - 1$. Moreover, $\epsilon_l^A \lambda_l^A = m_l/M_A$ (similarly for h), and $\epsilon_l^{Y^{--}} \lambda_l^{Y^{--}} = m_{E_l}/M_{Y^{--}}$.

In the cases with a singly or doubly charged scalar, there are also diagrams in which the photon is connected to the scalar line (see diagram b in Fig. 5.2). In the case of Y^{--} we obtain

$$\Delta a_\zeta^l(\zeta) = \frac{Q_\zeta}{8\pi^2} m_l^2 \frac{1}{M_\zeta^2} \int_0^1 dx \, \frac{|P_\zeta^l|^2 R_1^\zeta(x, \epsilon_l^\zeta) + |S_\zeta^l|^2 R_2^\zeta(x, \epsilon_l^\zeta)}{R^\zeta(x, \epsilon_l^\zeta, \lambda_l^\zeta)}, \tag{5.4}$$

for the scalar couplings. When $\zeta = Y^{--}$ we define

$$\begin{aligned} R_1^{Y^{--}}(x, \epsilon_l^{Y^{--}}) &= x[-(1-x) + \epsilon_l^{Y^{--}})], \\ R_2^{Y^{--}}(x, \epsilon_l^{Y^{--}}) &= x[1 - x + \epsilon_l^{Y^{--}}] \\ R^{Y^{--}}(x, \epsilon_l^{Y^{--}}, \lambda_l^{Y^{--}}) &= x[\lambda_l^2(x-1) + \left(\epsilon_l^{Y^{--}} \lambda_l^{Y^{--}}\right)^2] - (x-1). \end{aligned} \tag{5.5}$$

and when $\zeta = Y^-_{1,2}$ we have

$$\begin{aligned}
&R_1^{Y^-_{1,2}}(x,\epsilon_l^-) = -x(1-x),\\
&R_2^{Y^-_{1,2}}(x,\epsilon_l^{Y^-_{1,2}}) = x(1-x)\\
&R^{Y^-_{1,2}}(x,\epsilon_l^{Y^-_{1,2}},\lambda_l^{Y^-_{1,2}}) = (\lambda_l^{Y^-_{1,2}})^2(x-1)^2,
\end{aligned} \tag{5.6}$$

where we have neglected $\epsilon_\nu^{Y_1^-} = m_\nu/m_l$ for both electron and muon. In fact, we are neglecting the PMNS matrix and assuming for practical purposes that the ν-Y_1^--l vertex is diagonal. This means that we are over-estimating the contributions of the $Y^-_{1,2}$ scalar but even in this case we will see that their contributions are negligible.

5.2. Vector contributions

The model has neutral and doubly charge vector bosons that contribute to the AMDM in one loop, Z'_μ and U^{--}_μ, respectively. In the latter case, when the photon is connected to the charged vector line (diagram d in Fig. 5.2), we have:

$$\Delta a_U^l(U) = -\frac{G_{UUA}}{64\pi^2}\frac{m_l^2}{M_U^2}\int_0^1 dx\left[\frac{T_1(x,\epsilon_l^U)+T_2(x,\epsilon_l^U)+T_3(x,\epsilon_l^U)T(x,\epsilon_l^U,\lambda_l^U)}{T(x,\epsilon_l^U,\lambda_l^U)}\right], \tag{5.7}$$

with $\lambda_l^U = m_l/M_U$, where M_U is the mass of the U^{--}_μ; $\epsilon_l^U = m_I/m_l,\ E_I = E_e, E_\mu, E_\tau$. We have both vector and axial-vector couplings:

$$\begin{aligned}
T_1(x,\epsilon_l^u) &= |A_U^l|^2[h(x)+3\epsilon_l^U(x+1)] + |V_U^l|^2[h(x)+3\epsilon_l^U(x+1)]\\
T_2(x,\epsilon_l^U) &= \frac{m_l^2}{M_U^2}x^3[|A_U^l|^2(x+2\epsilon_l^U) + |V_U^l|^2(2\epsilon_l^U - x)],\\
T_3(x,\epsilon_l^U) &= 2|A_U^l|^2[h(x)+4+\epsilon_l^U(2x+1)] + |V_U^l|^2[-(2x+1)^2+\epsilon_l^U(6x+1)]\\
T(x,\epsilon_l^U,\lambda_l) &= x-1-x[(\lambda_l^U)^2(x-1)+(\epsilon_l^U\lambda_l^U)^2],
\end{aligned} \tag{5.8}$$

where we have defined $h(x) = 2x^2 + x - 3$.

The factor $G_{UUA} = -2e$, see Eq. (C.9), and A_U^l and V_U^l are given in Sec. C.4. There is only one diagram of this type, that with U^{--} in Fig. 5.1.

For the case where the photon is connected to the fermion line (diagram c in Fig. 5.2), there are two diagrams in Fig. 5.1 that contribute to the MDM, one with Z' and the other with U^{--}:

$$\Delta a_X^l(f) = -\frac{Q_I}{8\pi^2}m_l^2\sum_X\frac{1}{M_X^2}\int_0^1 dx\left[\frac{\tilde{R}_1^X(x,\epsilon_l^X)+\tilde{R}_2^X(x,\epsilon_l^X)+\tilde{R}_3^X(x,\epsilon_l^X)\tilde{R}^X(x,\epsilon_l^X,\lambda_l^X)}{\tilde{R}^X(x,\epsilon_l^X,\lambda_l^X)}\right], \tag{5.9}$$

where $X = Z'_\mu, U^{--}_\mu$, and$M$ is the mass of the vector boson, Q_I is the electric charge of the fermion internal in the loops, $\lambda_l^X = m_l/M_X$, with

$$\begin{aligned}
\tilde{R}_1^X(x,\epsilon_l^X) &= 2|A_X^l|^2(1+x+2\epsilon_l^X) + 2|V_X^l|^2(1+x-2\epsilon_l^X),\\
\tilde{R}_2^X(x,\epsilon_l^X) &= \frac{m_l^2}{M_X^2}(x-1)^2\left[|A_X^l|^2(1+\epsilon_l^X)(x-\epsilon_l^X) + |V_X^l|^2(1-\epsilon_l^X)(x+\epsilon_l^X)\right],\\
\tilde{R}_3^X(x,\epsilon_l^X) &= (3x-1)[|A_X^l|^2(1+\epsilon_l^X) + |V_X^l|^2(1-\epsilon_l^X)],\\
\tilde{R}^X(x,\epsilon_l^X,\lambda_l^X) &= 1+(x-1)[(\lambda_l^X)^2 + (\epsilon_l^X\lambda_l^X)^2].
\end{aligned} \tag{5.10}$$

In Eqs. (5.8) and (5.10), when $X = U^{--}_\mu$ the matrices A_U^l and V_U^l are those in Sec. C.4 and, when $X = Z'_\mu$, $A_{Z'}^l$ and $V_{Z'}^l$ are given by the factors f_A^l and f_V^l in Eq. (C.14). Notice that when the vector is the Z', $\epsilon_l^{Z'} = 1$. But with U^{--}_μ defined as above: $\epsilon_l^U = m_E/m_l$. For all the vertices the reader is referred to Appendices C.1 - C.5.

6. Results for the electron and the muon AMDM

Considering the results in the previous section, we are able to find sets of values for the parameters of the model taking into account the contributions of the scalars A^0, Y_1^-, Y^{++} and the vector bosons V_μ^-, U_μ^{--} for the electron and the muon AMDM. Let us define the contributions of the extra particles in the 331HL as in Eq. (5.1), where $\Delta a_{e,\mu}^{331}$ was calculated using the results from the previous section and considering all diagrams in Fig. 5.1, in such a way to obtain $\mu_{331} + \mu_{SM} = \mu_{exp}$ within 1 to 3 standard deviations.

6.1. Numerical results for the AMDMs

Here we will present the numerical results of the AMDMs for both, muon and electron, showing which regions of the parameter space satisfy the experimental results. We will consider five different scenarios, each with a different set of diagonalization matrices for the leptonic sector (see Appendix C.1 for more details). The unknown variables we have to explore are:

- The diagonalization matrices $V_{L,R}^l$ for the lepton mass matrices;
- The masses of the scalars A^0, $Y_{1,2}^+$ and Y^{++};
- The projections of the $Y_{1,2}^+$ scalars over its mass eigenstates;
- The masses of the exotic leptons E_e, E_μ and E_τ;
- The vacuum expectation value v_χ.

In the paragraph below we explain how each of these variables have been explored.

When the masses of the exotic particles are not explicitly mentioned in each plot, it means that they were fixed as: $m_{E_e} = m_{E_\mu} = m_{E_\tau} = 500$ GeV, $m_{Y_2^-} = 1200$ GeV and

$m_{A^0} = m_{Y^{--}} = m_{Y_1^-} = 1000$ GeV. Also, the projections of the singly charged scalars over its mass eigenstates were assumed to be both 0.5, see Eq. (C.3). We have tried several values for the scalar couplings, but they have given no noticeable change in our plots, that is because the U^{++} contribution dominates (see Fig. 6.1). The masses of the gauge bosons ($U^{\pm\pm}$ and Z') have their values defined by the value of $|v_\chi|$, since its other parameters are already fixed (see [42] for details). According to [1], the lowest lower limit on the mass of the Z' boson is 2.59 TeV, assuming it has the same couplings as the Z boson, which implies $|v_\chi| > 665.13$ GeV [35]. Here we will show that in the present model a stronger lower limit for v_χ is obtained and that, at least with the values of the matrices V_L^l used, it is not possible to fit both (1.3) and (1.4) at the same time within 1σ. For our fits, we considered only the uncertainties coming from the SM predictions and experimental results, for we have not calculated the 331HL contributions uncertainties.

6.1.1. Diagonal $V_{L,R}^l$ matrices

The simplest solution possible is to assume that the leptonic interactions are diagonal in flavor, i.e., the symmetry and mass eigenstates are the same, the numerical results for these matrices can be seen in Figs. 6.2-6.4. In Fig. 6.2 we vary the mass of the exotic lepton E_e, fixing the masses of the other two. The blue, green and cyan regions show values for the parameters where the 331HL-only contributions for the muon AMDM agrees with the difference between the experimental results and the SM prediction within 1σ - 3σ, respectively. In a similar manner, the red, orange and yellow regions show values where the 331HL-only contribution for the electron MDM agrees within 1σ, 2σ, and 3σ, respectively. It can be seen in the figure that there are solutions for the muon up to 1σ and for the electron up to 2σ. However the 1σ and 2σ regions only overlap for low values of m_{E_e}, less than 40 GeV, and v_χ around 80 TeV. These are not unrealistic solutions because an extra charged lepton lighter than 40 GeV may still exist depending of the respective couplings with the known particles, and v_χ may have a value of 60-80 TeV such that Z' and bileptons V, U will be only of a few tens of TeVs (See Eq. 6.9).

It is expected that high values for the exotic leptons and bosons masses would lead to results similar to the ones found in the SM, where the electron AMDM deviates from the experimental results by 1.1σ. It can be seen in Fig. 6.2 that, for values of v_χ over 60 TeV and $m_{Ee} \lesssim 1$ GeV, we have a 2σ region for the electron AMDM. Such high values for v_χ implies masses of tens of TeV's for the exotic gauge bosons, suppressing

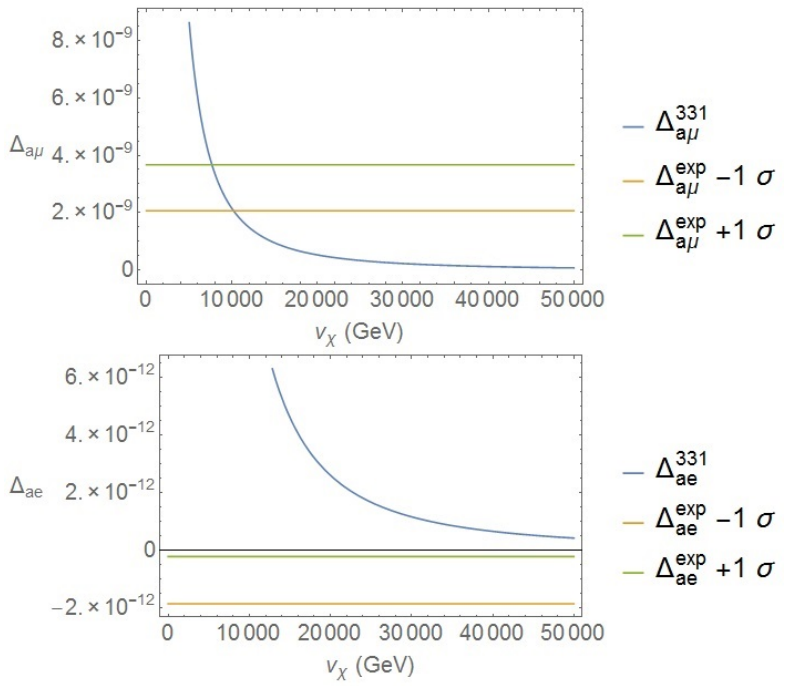

Figure 6.1.: U^{--} contribution to the muon AMDM. Δa_e (lower graph) and Δa_μ (upper graph) taking into account only the contribution of the doubly charged vector boson U^{--} as function of v_χ, with $0 < v_\chi \leq 50$ TeV. We also assume that both $V_{L,R}$ are the unit matrix and $m_{Ee} = m_{E\mu} = m_{E\tau} = 20$ GeV. It can be seen that the muon MDM is solved for v_χ around 8 TeV, a value that does not solve the electron MDM.

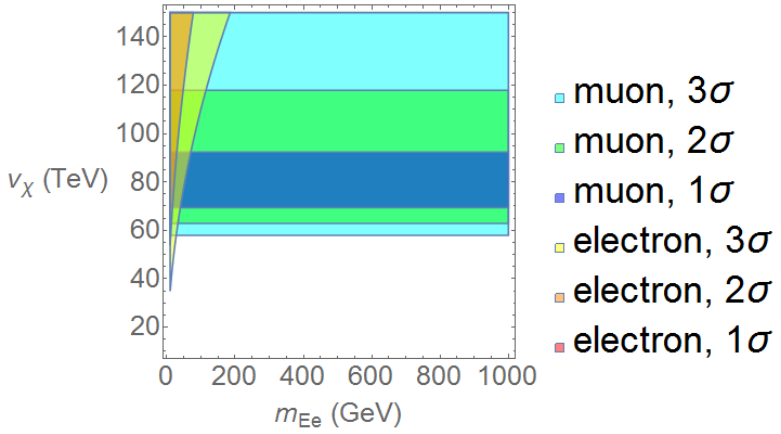

Figure 6.2.: v_χ and m_{E_e} values satisfying Eq. (5.1) within 1σ, 2σ and 3σ. Here we have used diagonal mass matrices for the charged leptons (see Sec. 6.1.1) and considered: $m_{E_\mu} = m_{E_\tau}$ =500, $m_{Y_2^+}$ =1200, and $m_{A^0} = m_{Y^{++}} = m_{Y_1^+}$ =1000 (all in GeV). The masses of the exotic gauge bosons ($U^{\pm\pm}$ and Z') have their values defined by the value of v_χ, since its other parameters are already fixed (see [42] for details).

several of the diagrams shown in Fig. 5.1, leaving us diagrams with exotic leptons and scalars. However, for the exotic lepton masses, we find a different situation. By analyzing Eqs. (5.2), (5.4), (5.7) and (5.9), we can see that if we take the limit $m_I \to \infty$ the expressions being integrated go to one. Therefore, the AMDM contributions coming from the diagrams with an exotic lepton inside their loops do not go to zero when these leptons are very heavy, leaving us with values that do not correspond to the ones expected by the SM, which would give us solutions for the electron AMDM within 2σ. Once we perform the AMDM calculations from the amplitudes involved, the integrations create this situation where the powers of m_I are the same in the denominator and numerator. The addition of these exotic leptons invaribly lead to contributions to the AMDM, regardless of its masses.

We have just considered diagonal interactions for the leptons so far, but we can use realistic unitary matrices which satisfy the condition $V_L^l M^l V_R^{l\dagger} = \mathrm{diag}(m_e\, m_\mu\, m_\tau)$ and the PMNS matrix. In the following sections we will consider four different parametrizations for these unitary matrices.

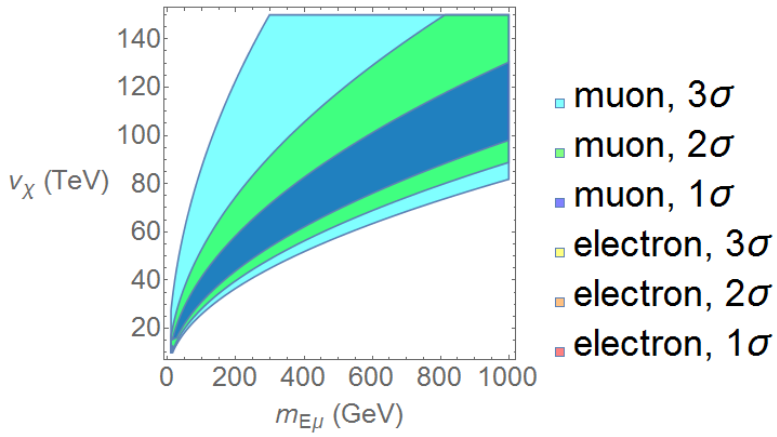

Figure 6.3.: Same as in Fig. 6.2 but now with $m_{E_e} = m_{E_\tau}$ =500 GeV.

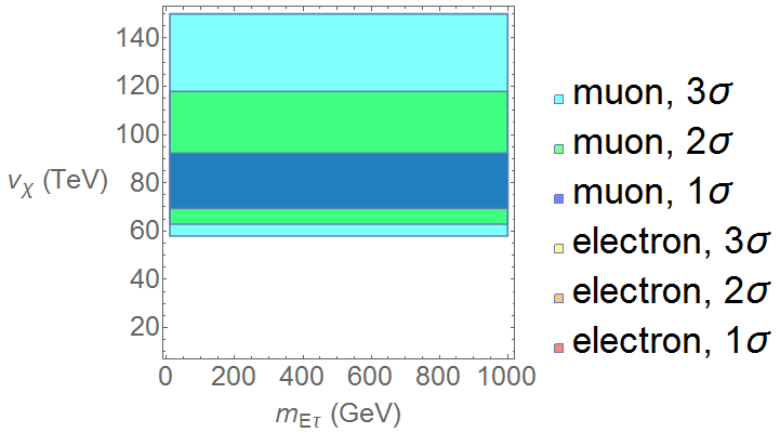

Figure 6.4.: Same as in Fig. 6.2 but now with $m_{E_e} = m_{E_\mu}$ =500 GeV.

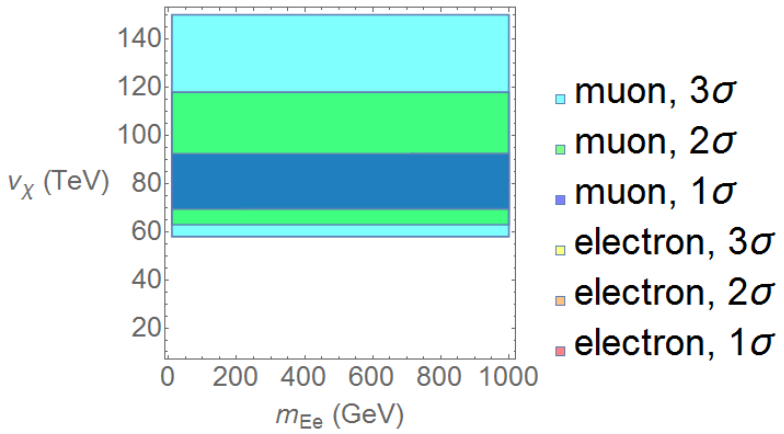

Figure 6.5.: v_χ and m_{E_e} values satisfying Eq. (5.1) within 1σ, 2σ and 3σ. Here we used the first set of diagonalization matrices (see Sec. 6.1.2) and considered: $m_{E_\mu} = m_{E_\tau}$ =500, $m_{Y_2^+}$ =1200, and $m_{A^0} = m_{Y^{++}} = m_{Y_1^+}$ =1000 (all in GeV). The masses of the exotic gauge bosons ($U^{\pm\pm}$ and Z') have their values defined by the value of v_χ, since its other parameters are already fixed (see [42] for details).

6.1.2. 1st set of $V^l_{L,R}$ matrices

The diagonalization matrices used in this set are:

$$V_L^l = \begin{pmatrix} 0.009854320681804862 & 0.31848228260886335 & -0.9478775912680647 \\ 0.014570561834801654 & -0.947868712966038 & -0.3183278211340082 \\ -0.9998452835772734 & -0.010674204623999706 & -0.013981068053858256 \end{pmatrix} \tag{6.1}$$

$$V_R^l = \begin{pmatrix} 0.005014143494893113 & 0.0026147097108665555 & 0.9999840107012414 \\ 0.0071578125624917055 & 0.9999708696847197 & -0.0026505662235414198 \\ 0.9999618113129783 & -0.0071709884334755225 & -0.004995281829296536 \end{pmatrix} \tag{6.2}$$

Figs. 6.5 and 6.6 shows us only solutions for the muon. Meanwhile, in Fig. 6.7 we have solutions for the electron up to 2σ. These solutions intersect with the 3σ solutions for the muon for values of m_{E_τ} smaller than 20 GeV and v_χ greater than 140 TeV. As for the 3σ solutions for the electron, they intersect the muon 2σ region for $m_{E_\tau} < 50$ GeV and $v_\chi \sim 90$ TeV.

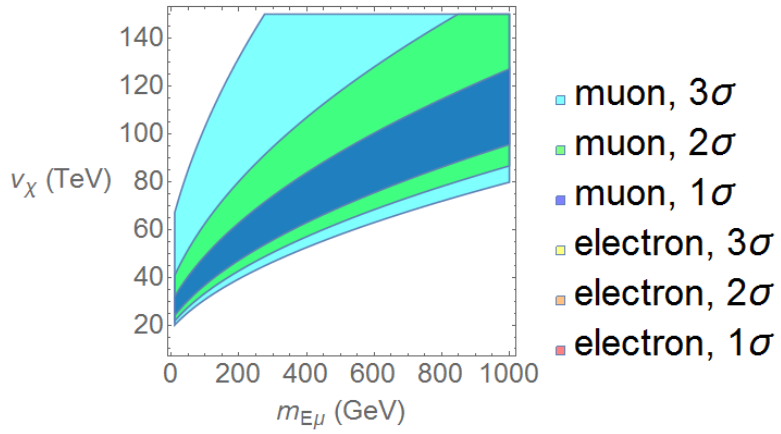

Figure 6.6.: Same as in Fig. 6.5 but now with $m_{E_e} = m_{E_\tau}$ =500 GeV.

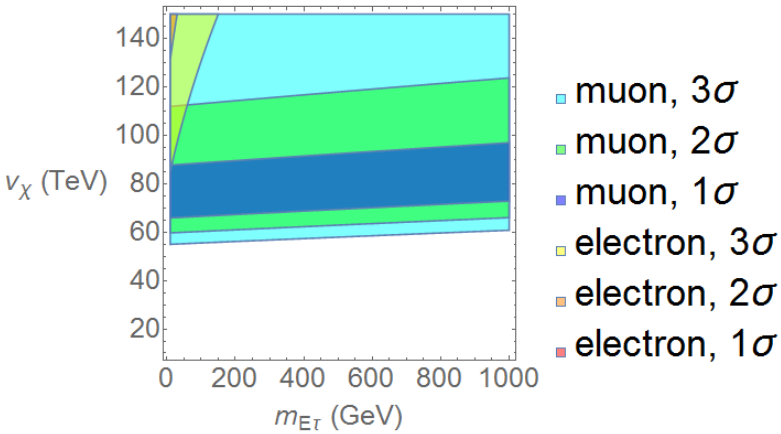

Figure 6.7.: Same as in Fig. 6.5 but now with $m_{E_e} = m_{E_\mu}$ =500 GeV.

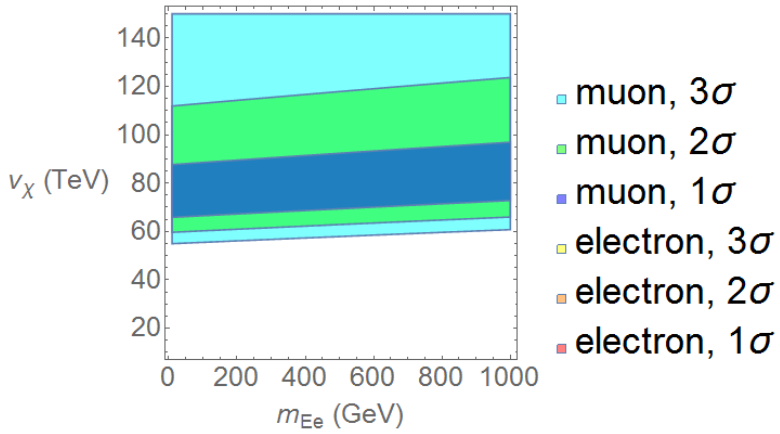

Figure 6.8.: v_χ and m_{E_e} values satisfying Eq. (5.1) within 1σ, 2σ and 3σ. Here we used the second set of diagonalization matrices (see Sec. 6.1.3) and considered: $m_{E_\mu} = m_{E_\tau}$ =500, $m_{Y_2^+}$ =1200, and $m_{A^0} = m_{Y^{++}} = m_{Y_1^+}$ =1000 (all in GeV). The masses of the exotic gauge bosons ($U^{\pm\pm}$ and Z') have their values defined by the value of v_χ, since its other parameters are already fixed (see [42] for details).

6.1.3. 2nd set of $V_{L,R}^l$ matrices

The diagonalization matrices used in this set are:

$$V_L^l = \begin{pmatrix} -0.009 & 0.0146 & -0.9998 \\ -0.3185 & -0.9479 & -0.0107 \\ 0.9479 & -0.3183 & -0.0140 \end{pmatrix} \tag{6.3}$$

$$V_R^l = \begin{pmatrix} 0.005 & 0.0072 & 0.9999 \\ 0.0026 & 0.9910 & -0.0072 \\ 0.9999 & -0.0027 & -0.0050 \end{pmatrix} \tag{6.4}$$

Similar to the first set of matrices, the plots where we vary m_{E_e} and m_{E_μ} (Figs. 6.8 and 6.9) show only muon solutions, while in Fig. 6.10 have solutions for both electron and muon that overlap. The situation is similar to the 1st set of matrices, now with a broader range of values for v_χ. Better than before, now the 2σ electron region and the 1σ muon region are overlapping, for values of $m_{E_\tau} \lesssim 15$ GeV and $v_\chi \sim$80 TeV.

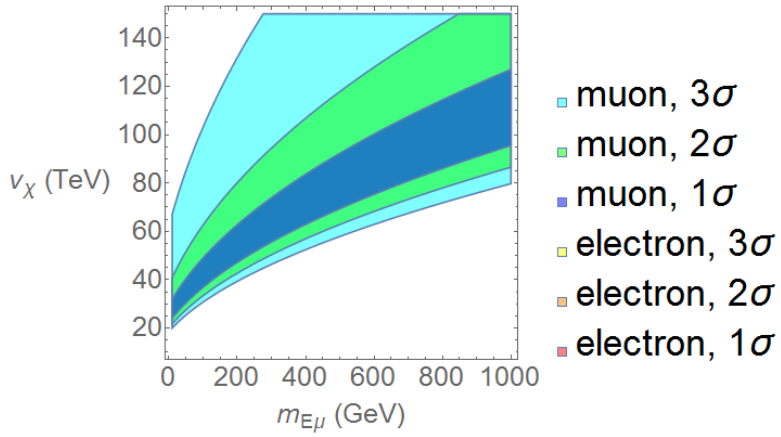

Figure 6.9.: Same as in Fig. 6.8 but now with $m_{E_e} = m_{E_\tau}$ =500 GeV.

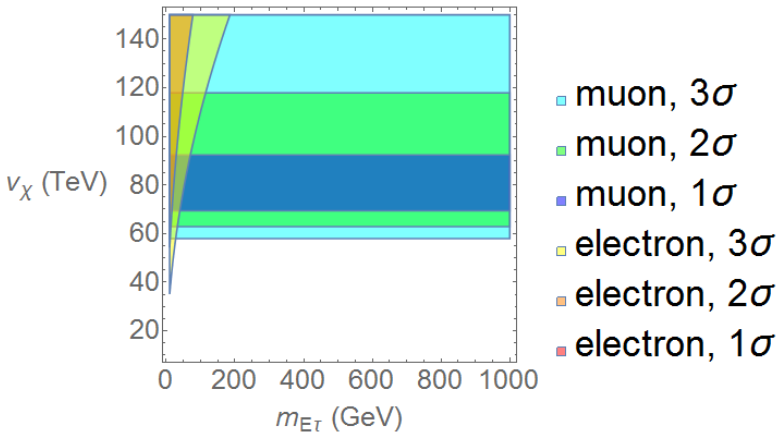

Figure 6.10.: Same as in Fig. 6.8 but now with $m_{E_e} = m_{E_\mu}$ =500 GeV.

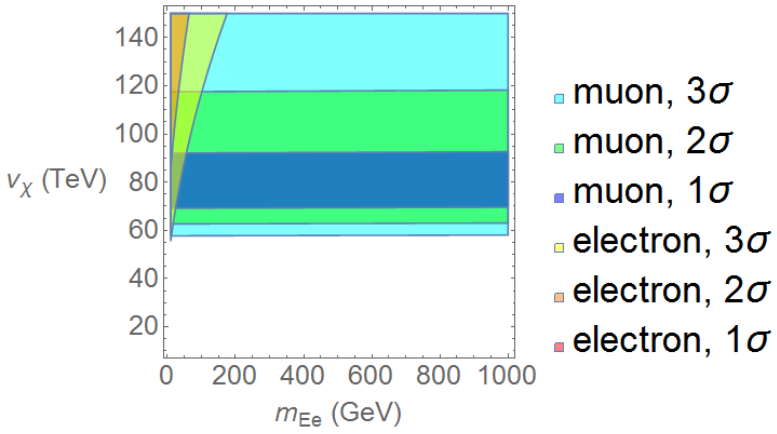

Figure 6.11.: v_χ and m_{E_e} values satisfying Eq. (5.1) within 1σ, 2σ and 3σ. Here we used the third set of diagonalization matrices (see Sec. 6.1.4) and considered: $m_{E_\mu} = m_{E_\tau}$ =500, $m_{Y_2^+}$ =1200, and $m_{A^0} = m_{Y^{++}} = m_{Y_1^+}$ =1000 (all in GeV). The masses of the exotic gauge bosons ($U^{\pm\pm}$ and Z') have their values defined by the value of v_χ, since its other parameters are already fixed (see [42] for details).

6.1.4. 3rd set of $V_{L,R}^l$ matrices

The diagonalization matrices used in this set are:

$$V_L^l = \begin{pmatrix} 0.983908 & 0.156151 & 0.086891 \\ 0.0777852 & 0.061974 & -0.994965 \\ -0.160853 & 0.985709 & 0.0500342 \end{pmatrix} \tag{6.5}$$

$$V_R^l = \begin{pmatrix} 0.978756 & 0.186555 & 0.0850542 \\ 0.0744144 & 0.0633254 & -0.99215 \\ -0.191048 & 0.980401 & 0.0480978 \end{pmatrix} \tag{6.6}$$

In this set only Fig. 6.11 has solutions for the muon and the electron. The 2σ regions for the electron and muon overlap for $m_{E_e} \lesssim 30$ GeV and $v_\chi \sim 110$ TeV. Also, there is an overlap of the electron 3σ and the muon 1σ regions, for $m_{E_e} \lesssim 50$ GeV and $v_\chi \sim 80$ TeV.

6.1.5. 4th set of $V_{L,R}^l$ matrices

The diagonalization matrices used in this set are:

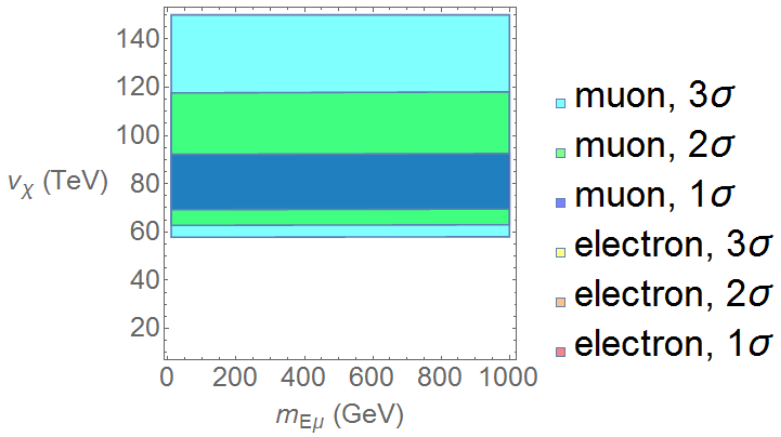

Figure 6.12.: Same as in Fig. 6.11 but now with $m_{E_e} = m_{E_\tau}$ =500 GeV.

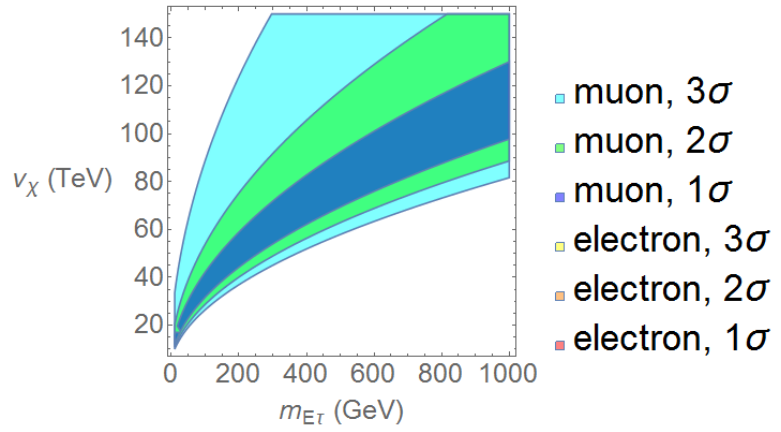

Figure 6.13.: Same as in Fig. 6.11 but now with $m_{E_e} = m_{E_\mu}$ =500 GeV.

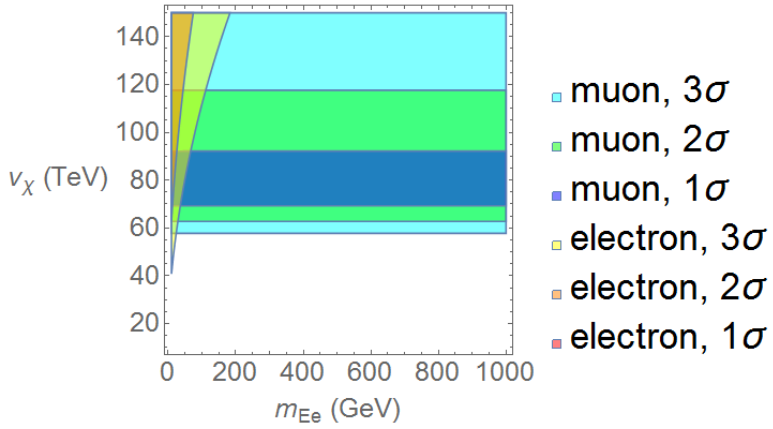

Figure 6.14.: v_χ and m_{E_e} values satisfying Eq. (5.1) within 1σ, 2σ and 3σ. Here we used the fourth set of diagonalization matrices (see Sec. 6.1.5) and considered: $m_{E_\mu} = m_{E_\tau}$ =500, $m_{Y_2^+}$ =1200, and $m_{A^0} = m_{Y^{++}} = m_{Y_1^+}$ =1000 (all in GeV). The masses of the exotic gauge bosons ($U^{\pm\pm}$ and Z') have their values defined by the value of v_χ, since its other parameters are already fixed (see [42] for details).

$$V_L^l = \begin{pmatrix} -0.99614 & -0.08739 & -0.00826 \\ 0.01357 & 0.24625 & -0.96691 \\ 0.08672 & 0.96526 & 0.24649 \end{pmatrix} \tag{6.7}$$

$$V_R^l = \begin{pmatrix} 0.99624 & -0.08629 & -0.00801 \\ 0.01179 & 0.226594 & -0.97392 \\ 0.08586 & 0.97016 & 0.22676 \end{pmatrix} \tag{6.8}$$

In Fig. 6.14 we see solutions for the muon and electron that overlap for low values of m_{E_e}, while in Figs. 6.15 and 6.16 we see only solutions for the muon. The situation in Fig. 6.14 is similar to that in Fig. 6.10, where the 2σ electron region and the 1σ muon region are overlapping, for values of $m_{E_\tau} \lesssim 15$ GeV and $v_\chi \sim$80 TeV.

6.2. Numerical analysis conclusions

Although we considered all the contributions to the $\Delta a_{e,\mu}$ in 1-loop in all these scenarios, assuming different sets of diagonalization matrices for the leptonic sector, it is easy to convince ourselves that the larger ones come from the doubly charged scalar Y^{--} and

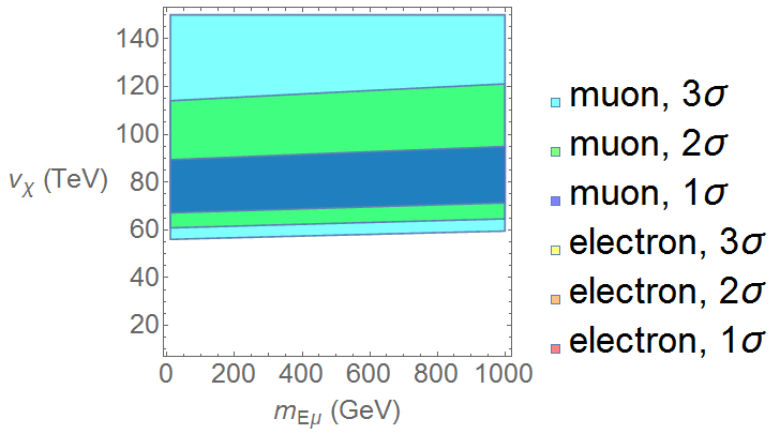

Figure 6.15.: Same as in Fig. 6.14 but now with $m_{E_e} = m_{E_\tau}$ =500 GeV.

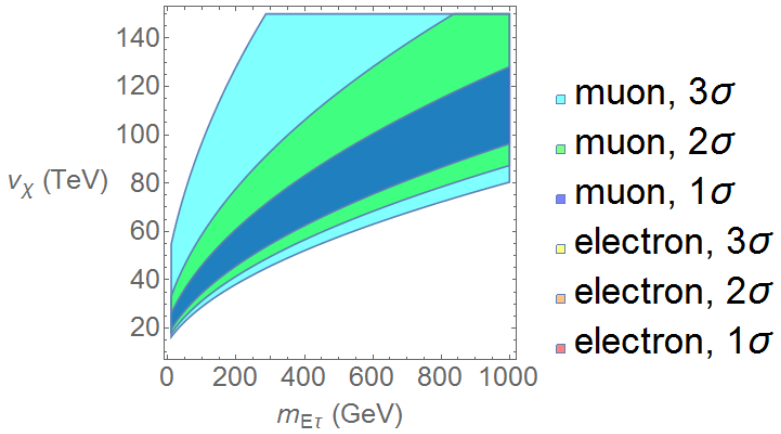

Figure 6.16.: Same as in Fig. 6.14 but now with $m_{E_e} = m_{E_\mu}$ =500 GeV.

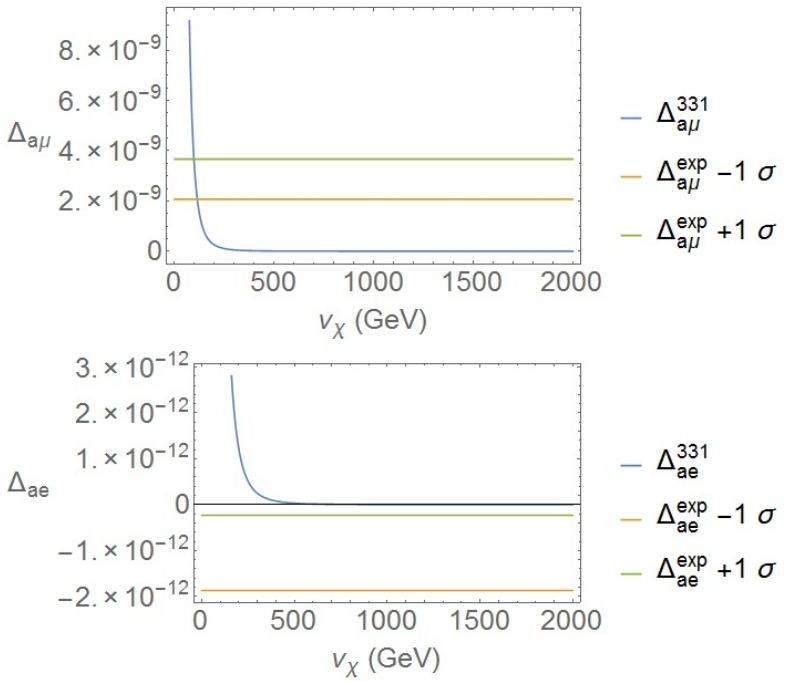

Figure 6.17.: Y^{--} contribution to the muon MDM. Δa_e (lower graph) and Δa_μ (upper graph) taking into account only the contribution of the doubly charged scalar Y^{--} as function of v_χ, with $0 < v_\chi \leq 2$ TeV, $m_{Y^{--}} = 500$ GeV. We also assume that both $V_{L,R}$ are the unit matrix and $m_{Ee} = m_{E\mu} = m_{E\tau} = 20$ GeV. We see that the muon MDM only has solutions for $v_\chi \approx 100$ GeV, while the electron MDM has no solutions for this value.

vector U^{--} (see Figs. 6.17 and 6.1). In fact, from the vertices in Eq. (C.2), we can see that the contributions of the neutral scalar are suppressed since they are proportional to the known charged lepton masses $(\hat{M}^l/v_\rho)O_{\rho 1}$. The pseudo-scalar vertex is proportional to $(\hat{M}^l/v_\rho)U_{\rho 3}$, thus may be larger than the scalar one but still very suppressed. The vertex of the singly charged scalar Y_1^- is also proportional to $(\hat{M}^l/v_\rho)$, and in this case there are additional suppression factors $\cos\beta V_L^l$, see Eq. (C.3). Given that the singly charged scalar contribution is negligible, the introduction of the a_{10} term in the scalar potential bring no significant change to our results, but it is necessary for the width decay of the leptons E^+.

In the case of the doubly charged scalar Y^{--}, it has interactions proportional to $\hat{M}^E/v_\rho > 1$, see Eq. (C.4). Finally, we note that the doubly charged vector bilepton,

U^{--} has vertices that are proportional to $gV_L^{l\dagger} = (4G_F M_W^2/\sqrt{2})^{1/2} V_L^{l\dagger}$, see Eqs. (C.12) and (C.13). Hence, our results also depend on the values of the matrices V_L^l, which we considered.

Most studies of the possibilities of the 3-3-1 models for solving the muon anomaly have considered that the interactions are diagonal in flavor, the scenario we addressed in Sec. 6.1.1. These authors obtain solutions with low masses for the particles in their models. These interactions are characterized by a coupling strength denoted by f in Ref. [3] from where some authors take off the results for the Feynman diagrams. However, in a particular model, the mass eigenstates appear only after diagonalizing the mass matrices, in doing so the coupling strength f is related to masses of the internal particles in the diagrams and to the unitary matrices that diagonalize the mass matrices. Thus, they are not anymore arbitrary. Moreover, in most works studying Δa_μ, usually only one type of exotic particle is considered to address the problem.

To make a comparison, we have calculated the contributions given only by U^{--} and Y^{--} (Figs. 6.17 and 6.1) considering diagonal interactions (i.e. $V_{L,R}^l = 1$). When considering only the vector U^{--}, although it solves the muon anomaly for v_χ around 8 TeV, this does not happen for the electron AMDM around the same value. From the bottom plot in the same figure, it seems that the electron AMDM can be solved for higher values of v_χ, but these values will not satisfy the muon AMDM according to the upper plot. For the case where only Y^{++} contributes, the muon AMDM is solved for $v_\chi \approx 100$ GeV while the electron is not solved for this value. So it seems that even with diagonal interaction the AMDMs cannot be solved simultaneously.

Of course, our results are in the 331HL model and are not necessarily valid in other 331 models, and also for other values of the matrix V_L^l. However they indicate that the analysis in those models should be revisited. Not just because diagonal flavor interactions were the only ones considered, but also because of the effects that these exotic particles may have on the electron AMDM. The effects on both AMDMs can be contradictory, as we have shown in this work.

Once we have determined the value of the VEV v_χ we can calculate the vector boson

masses [42] and m_E using:

$$M_U^2 \approx \frac{\alpha}{4s_W^2}(v_\rho^2 + v_\chi^2), \quad M_V^2 \approx \frac{\alpha}{4s_W^2}(v_\eta^2 + v_\chi^2)$$
$$M_{Z'}^2 = \frac{\alpha^2}{2s_W^2}\frac{(1-2s_W^2)(4+\bar{v}_W^2) + s_W^4(4-\bar{v}_W^2)}{6c_W^2(1-4s_W^2)}$$
$$m_{E_l} = g_{E_l}\frac{v_\chi}{\sqrt{2}}, \tag{6.9}$$

where $\bar{v}_W = v_{SM}/v_\chi$, and we see that with $v_\chi = 70$ TeV we have $M_U \approx 22$ TeV, $M_V \approx 22$ TeV, $M_{Z'} \approx 81$ TeV.

On the other hand, the masses of the scalars $Y_{1,2}^-, Y^{--}$ depend also on the dimensionless couplings appearing in the scalar potential, and also on the trilinear term in the scalar potential, $F\,\eta\rho\chi$ denoted by α in [34]. The constant F, with dimension of mass, may be small on naturality grounds, or large if it arises from the VEV of a heavy neutral scalar that is singlet under the 3-3-1 symmetry. For this reason the masses of the scalars $A, Y_{1,2}^-, Y^{--}$ and m_{E_l} are used as inputs in our calculations. On the other hand, the masses of the vectors Z', V^-, U^{--} depend mainly on v_χ, since the other VEVs are already fixed.

7. Other constraints

In the previous chapter we were able to find some solutions for the AMDMs, all of them requiring low values for the exotic lepton mass, below 50 GeV. The current experimental lower limits for exotic leptons are around 100 GeV, excluding our solutions. However, such limits were obtained considering models different from the 3-3-1 model with heavy leptons, which, in principle, cannot be directly applied to our case. Also, we explore the $\mu \to e\gamma$ decay, which excluded one of our numerical solutions for the lepton diagonalization matrices. In the following sections we further discuss these topics.

7.1. The $\mu \to e\gamma$ decay

One possible constraint on the m_E and v_χ values can come from the $\mu \to e\gamma$ decay. The diagrams contributing to this process are those in Fig. 5.1 when the intermediate fermions are E's ou neutrinos and we have a muon and an electron at the external lines. These processes have been considered recently in the context of the minimal 3-3-1 model [37] and an early reference is Ref. [44]. Considering only the largest contribution for the branching ratio to this process, we have

$$BR(\mu \to e\gamma) = \frac{54\alpha}{\pi}\left(\frac{m_U}{m_{Y_1}}\right)^4\left(\frac{m_E}{m_\mu}\right)^2\left(|(V_Y)_{13}|^2|(V_Y)_{32}|^2 + |(V_Y)_{31}|^2|(V_Y)_{23}|^2\right) \quad (7.1)$$

where $V_Y = (V_R^l)^T V_L^l$ and α is the fine-structure constant. The actual experimental limit for this is $BR(\mu \to e\gamma) < 0.057 \times 10^{-11}$ [1]. Imposing this limit on the above equation, while varying m_E from 0 to 1000 GeV and v_χ from 10 to 150 TeV, considering all the sets of diagonalization matrices from the sections above, we saw that the whole range of values explored is allowed for the diagonal matrices, the first, second and fourth sets of matrices. As for the third set of matrices, none of the values explored for m_E and v_χ respects the experimental limit for the $\mu \to e\gamma$ decay branching ratio. Given the simplicity of these results, we decided not to show the respective plots here.

7.2. Lifetime of the exotic charged leptons

The experimental searches of new charged leptons have considered three scenarios in order to put constraints on the masses of this sort of particles [1]: i) sequential heavy leptons, in which these particles are assumed to belong to a fourth generation where either the neutrino partner is considered stable or the heavy leptons decay into active neutrinos via mixing; ii) stable heavy charged leptons, which considers the decay $L^{\pm} \to W^{\pm}\nu$ (where L is the exotic lepton); and iii) long lived heavy charged leptons, which considers an exotic lepton coming from a singlet added to the SM. None of these scenarios correspond to the 331HL case. In situation i) the lower limit on the mass of such particle is 100.8 GeV; in ii) it is 102.6 GeV, and finally in case iii) it is 574 GeV.

In the 331HL the heavy leptons $E^{\pm}$ are not stable but may be long-lived depending on the their masses and on the masses of the scalar bosons that mediate their decays. In particular, we note that the lower limit on the mass of a sequential heavy charged lepton, 100.8 GeV at 95%, was obtained using the decay $L^{\pm} \to W^{\pm}\nu$ [1]. However, in the present model, the decays are mediated mainly by extra charged vector and scalar bosons and, for this reason, it is not straightforward to apply this limit on the masses of $E^{\pm}$ in the present model.

The lepton triplets in terms of the symmetry eigenstates (primed fields) are $\Psi_{aL} = (\nu'_a\, l'_a\, E'_a)^T \sim (1,3,0)$, $a = e,\mu,\tau$ [31]. Usually it is assumed that the leptons E_a^+ are antiparticles and thus $L(E_a^+) = -1$. In this case the L assignment is

$$L(J, j, \eta_2^-, \chi^-, \chi^{--}, \rho^{--}, V_\mu^-, U_\mu^{--}) = +2. \tag{7.2}$$

and the other particles having $L = 0$, or $+1$. In this case the model has a global custodial symmetry $U(1)_L$ under which some particles (including the usual ones) are $L = 1$ (antiparticles $L = -1$) and the other ones as in Eq. (7.2). We can also use the global symmetry $U(1)_F$, where $F = B + L$ [39].

However, we can assume that the leptons E_a^+ are particles, as in Konopinski-Mahmoud [40], and assign it $L(E_a^+) = +1$. In this case the lepton number is the same for all members in lepton triplets, and $L(J, j, \eta_2^-, \chi^-, \chi^{--}, \rho^{--}, V_\mu^-, U_\mu^{--}) = 0$. Notwithstanding, a custodial discrete $\mathbb{Z}_2$ symmetry still exists, under which $E, J, j, \eta_2^-, \chi^-, \chi^{--}, \rho^{--}, V_\mu^-, U_\mu^{--}$ are odd, and the rest of the particles are even. The electroweak symmetry of the model is $G_W = \mathbb{Z}_2 \times SU(3)_L \otimes U(1)_X$. In this section we call "exotic" the particles that are odd under $\mathbb{Z}_2$, otherwise they are "normal" particles. Now, $\mathbb{Z}_2$ is the custodial symmetry.

At first sight, the custodial discrete symmetry implies that the lightest exotic charged lepton should be stable. There are interactions that produce $E^+ = V^+\nu_L$ and $E^+ = U^{++}l^-$ but both vectors, V^+ and U^{++}, cannot decay only into known quarks or leptons: $U^{++} = E^+e^+$ and $V^+ = e_L^+\nu_R^c$. Moreover, these vector bosons can also decay into one exotic quark and one known quark, $V^+ = \bar{u}J$ and $U^{++} = u\bar{j}$. We can see from Eq. (4.9), that the interactions with charged scalars are similar, they involve also one normal and one exotic particle: $E_L^+ = \eta_2^+\nu_R$ and $E_R^+ = \nu_L\chi^+$, which are allowed since η_2^+ and χ^+ are odd under $\mathbb{Z}_2$. However, η_2^+ and χ^+ decays also into one normal particle and one exotic one. Hence, the lightest E^+ cannot, at first sight, decay at all.

However, we note that the quartic term $a_{10}(\chi^\dagger\eta)(\rho^\dagger\eta)$ is allowed in the scalar potential and it implies a mixing among all the singly charged scalars [41] (See appendix A):

$$V(\eta,\rho,\chi) \supset a_{10}(\chi^+\eta^0 + \chi^{++}\eta_1^- + \chi^{0*}\eta_2^+)(\rho^-\eta^0 + \rho^{0*}\eta_1^- + \rho^{--}\eta_2^+). \tag{7.3}$$

Notice that the term $\chi^+\eta^0\rho^-\eta^0$ breaks the $\mathbb{Z}_2$ symmetry. If $a_{10} \neq 0$, all the singly charged scalars mix in the mass matrix and since the interaction $\bar{\nu}_L E_R\chi^-$ does exist, the decay $E_{lR}^+ = \nu_{lL} + h^+ = \nu_{lL} + l^+ + \nu_l^c$ is now allowed, where h^+ is a charged scalar mass eigenstate that couples with the known leptons (we have omitted the matrix element that projects χ^+ onto h^+). The decay of any E through charged scalars is shown in Fig. 7.1. A rough calculation of the decay, based on the result for the muon decay $\mu \to 2\nu + e$, is given by

$$\tau_E = \frac{m_Y^4}{(Cm_E)^4}\frac{12(8\pi)^3}{m_E}\hbar, \tag{7.4}$$

where m_Y is the mass of the lightest singly charged scalar, and C denotes the couplings between the Y scalar and the fermions. In section 6.1 we assumed $m_{Y_1^+} = m_{Y_2^+} = 1000$ GeV, using this with Eq. 7.4, and assuming $C = 0.1$, we plot the graph in Fig. 7.2. We see that for values as low as 50 GeV for m_E, the lifetime is lower than 10^{-11} seconds. If we take $m_E = 10$ GeV, the lifetime is just 1.26×10^{-8} seconds, still very short and far from stable.

The channel into one charged lepton and two active neutrinos is open even for the lightest of the leptons E_a^+, and thus they are not long lived anymore. The issue of the stability of exotic fermions deserves a more detailed study that goes beyond the scope of this work. However, the above discussion tells us that the current experimental data is not applicable, at least in a straightforward way, to the 3-3-1 model with heavy leptons.

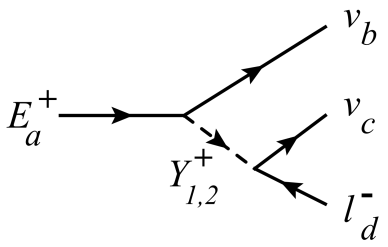

Figure 7.1.: E lepton decay. This decay is allowed even for the lightest lepton E.

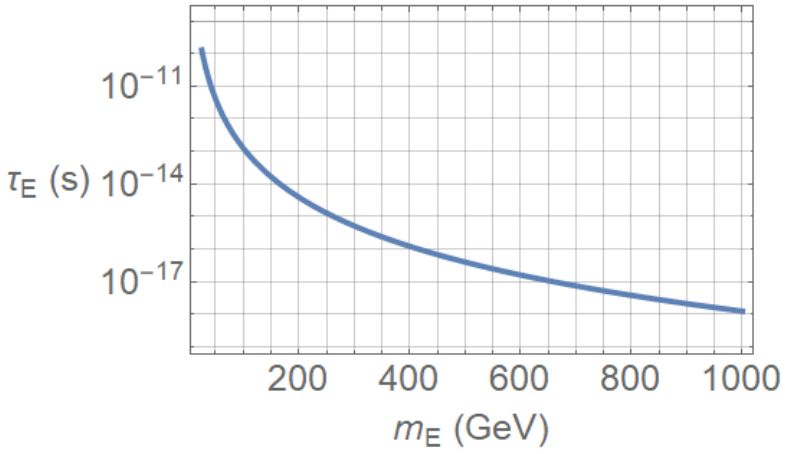

Figure 7.2.: E lepton lifetime, as described by Eq. 7.4. In the vertical axis we have the lepton lifetime in seconds, and on the horizontal axis the lepton mass in GeV.

8. Conclusions

In this work we have shown the analytical and numerical results for the electron and muon AMDM at 1-loop level in the 331HL model, comparing them with the experimental results. In the parameter space that has been explored here we have found regions where only the muon AMDM coincides with the experimental value whithin 1σ, while for the electron case only solutions within 2σ and 3σ were found. Moreover, even when we found solutions for both electron and muon, the region where they overlapped required very low mass values for the exotic leptons, and this may be a very unlikely scenario. We recall that the masses of vectors Z' and U^{--} are determined mainly by v_χ once the other VEVs are already fixed, but for the heavy scalars their masses, as for the heavy leptons, also depend on unknown dimensionless parameters. In this vein, we have used the charged scalars and heavy leptons masses as free inputs in our calculations.

The dominant contributions are due to Y^{--} and mainly to U^{--}. This can be appreciated in Figs. 6.17 and 6.1, respectively. We can see from these figures that, even in these two cases, it is impossible to fit in 1σ both Δa_e and Δa_μ. At 3σ for the electron and less than 2σ for the muon it is possible to have an agreement with the experimental measurements. However, it leaves the electron case in the same footing as the muon AMDM in the SM. For this reason we claim that it is not possible to fit both $\Delta_{e,\mu}$ at the same time. For most of the values explored for the parameters, the contributions of the a_e^{331} increase the value of Δa_e.

Other recent works have addressed the muon AMDM in different but similar scenarios, in which smaller values for v_χ and smaller masses for the extra particles were enough to explain the Δa_μ [6, 8, 9, 10, 11, 12, 13, 14, 15, 16, 17, 18]. However, none of them have considered at the same time the contributions for the electron AMDM from the particles and parameters that solve the muon AMDM.

One important difference with other works in 3-3-1 models is that usually the integrals from the Feynmann diagrams were taken from Ref. [3]. However, the results in the latter paper are quite general and do not take into account details that are model dependent.

For instance, they used directly the symmetry eigenstates basis, and in this situation the unitary matrices needed to diagonalize the lepton mass matrices do not appear in the vertices (nor does the VEVs that come from the diagonalization of the scalar mass matrices). Each contribution to the Δa_μ coming from new particles were given just as follows:

$$\Delta a_\mu = \pm \frac{f^2}{4\pi^2}\frac{m_\mu^2}{M^2} I, \tag{8.1}$$

where M is a mass of one of the particles in the loop and I an integral on the Feynman parameter x, also depending on parameters as ϵ and λ defined in Sec. 6. In some of the references above, this integral is simplified, turning into a numerical factor.

Besides that, in these works all vertices are reduced to the exotic particle with mass M, coupling to muons with coupling strength f. In our case, the mass eigenstates particles in the diagrams are obtained from the symmetry eigenstates and the unitary matrices relating both basis appear in the vertices. Here these matrices are incorporated in the factors S, P when the fields are (pseudo)scalars and V and A when they are the vectors.

For instance, in Ref. [6] the masses of all internal fermions in the loops are neglected in the reduced m331 model. This could be done because in this model the only internal fermions are the known leptons. In the m331 model (reduced or not) the interactions with the doubly charged scalar or vector boson have non-diagonal vector and axial-vector interactions that have not been considered in most works mentioned above. Moreover, in [6] the only mixing matrix in the lepton sector is the PMNS. The effect of this matrix is nullified by the small neutrino masses and the unitarity of the PMNS matrix. On the other hand, in the minimal 3-3-1 the charged current coupled to U^{++} is

$$\mathcal{L}_{ll}^{cc} = -i\frac{g}{2\sqrt{2}}\bar{l}^c\gamma^\mu[(V_U - V_U^T) - \gamma_5(V_U + V_U^T)]lU_\mu^{++} + H.c. \tag{8.2}$$

where $l = (e, \mu, \tau)^T$ and $V_U = (V_R^l)^T V_L^l$. We see that there are non-diagonal vector currents and the unitary matrices are such that $V_L^{l\dagger} M^l V_R^l = \hat{M}^l = \mathrm{diag}(m_e, m_\mu, m_\tau)$, it is an extreme fine tuning to assume that V_U is the unit matrix. Hence, in the minimal 331 model it is not advisable to neglect the lepton mixing.

In the model explored in this work this type of current involves E and l, and V_L^l, see Eq. (C.12). For instance, in [46] it is shown that the doubly charged scalar may solve the muon anomaly, using scalars with masses around hundreds of GeV's. The scheme in [46] could, at first sight, be realized in the m331. It is so because in that model, a singlet doubly charged scalar (under the SM symmetries) belonging to sextet couples only with

right-handed charged leptons, i.e., the respective interactions are $\overline{(l_R)^c}V_L^{lT}G^SV_R^l l_R$, where G^S is the Yukawa matrix in the interactions of leptons with the scalar sextet. Moreover, G^S is not proportional to the charged lepton masses because they have another source of mass: the interactions with the triplet η. Hence, the arbitrary matrix $V_L^{lT}G^SV_R^l$ has to be taken into account in the m331.

Another example, in Ref. [8], were considered solutions to the muon anomaly in the context of the minimal 331, the 331 model with heavy neutral fermions, and the 331 model with heavy charged leptons but with five left-handed lepton triplets, thus the latter one is different from the 331HL model here considered. Again, the results are all approximated and since all flavor mixings are neglected their results are, as before, of the form $\Delta a_\mu \propto m_\mu^2/M^2$. The masses of the usual charged leptons can be neglected in the loops because they appear as $\epsilon_\mu = m_\nu/m_\mu$ or $\lambda_l = m_\mu/M$. The first is negligible by the neutrino masses and the second by the value of M. Another important point to be stressed is that, in [8, 9] not all the particles in each model are considered. Moreover, it happens that in the model they were considering, the importance of the scalar contributions cannot be neglected *a priori* because they depend on the Yukawa couplings through the unitary matrices that diagonalize quarks and lepton mass matrices, as discussed in the previous paragraph. For instance, in the m331 there are FCNC via the scalar sector, and in this case the scalar contributions may be as important as in the quark sector [35].

We must put in context our results. On one hand, they were obtained in the 331HL where there are no flavor changing neutral interactions in the lepton sector. Moreover, unlike in the m331, the singly charged vector bilepton V^+ does not contribute to the AMDM of the known charged leptons. For example, this is not the case with the m331, where there are more scalar multiplets and FCNC in the lepton sector via the exchange of neutral scalars. On the other hand, they were obtained using the matrices V_L^l in Sec. 6.1. The matrices V_R^l which we presented are possible solutions, they may have other values and it is possible that these values might imply solutions for both AMDMs. The moral of the story is that besides the unitary matrices, the AMDM of the electron must be taken into account when solutions for the muon case are proposed, once both AMDMs may be incompatible. Otherwise, the results cannot be considered definitive because they depend also on the solutions for the matrices $V_{L,R}^l$ and different solutions imply different lower bounds on the phenomenology of the model [37].

A. Scalar Potential

The most general scalar potential is given by

$$\begin{aligned} V(\chi,\eta,\rho) &= \mu_1^2\chi^\dagger\chi + \mu_2^2\eta^\dagger\eta + \mu_3^2\rho^\dagger\rho + (\alpha\,\epsilon_{ijk}\chi_i\rho_j\eta_k + H.c.) + a_1\left(\chi^\dagger\chi\right)^2 \\ &+ a_2\left(\eta^\dagger\eta\right)^2 + a_3\left(\rho^\dagger\rho\right)^2 + a_4\left(\chi^\dagger\chi\right)\left(\eta^\dagger\eta\right) + a_5\left(\chi^\dagger\chi\right)\left(\rho^\dagger\rho\right) \\ &+ a_6\left(\rho^\dagger\rho\right)\left(\eta^\dagger\eta\right) + a_7\left(\chi^\dagger\eta\right)\left(\eta^\dagger\chi\right) + a_8\left(\chi^\dagger\rho\right)\left(\rho^\dagger\chi\right) \\ &+ a_9\left(\rho^\dagger\eta\right)\left(\eta^\dagger\rho\right) + a_{10}[(\chi^\dagger\eta)(\rho^\dagger\eta) + (\eta^\dagger\chi)(\eta^\dagger\rho)] \end{aligned} \tag{A.1}$$

we have assumed a_{10} real. The scalar potential with $a_{10} = 0$ has been considered for instance in Ref. [41, 34]. In the following sections we present the mass eigenstates for the scalars in the model.

B. Scalar mass eigenstates

From the scalar potential, presented in Eq. 4.8, we can find its minima conditions from its derivatives. Therefore, when taking $\partial V/\partial v_\chi = \partial V/\partial v_\rho = \partial V/\partial v_\eta = 0$ we obtain

$$\mu_1^2 = -\frac{1}{v_\chi}\left(a_1 v_\chi^3 + \frac{1}{2}a_4 v_\eta^2 v_\chi + \frac{1}{2}a_5 v_\rho^2 v_\chi - \frac{\alpha v_\eta v_\rho}{\sqrt{2}}\right), \tag{B.1}$$

$$\mu_2^2 = -\frac{1}{v_\eta}\left(a_2 v_\eta^3 + \frac{1}{2}a_4 v_\eta v_\chi^2 + \frac{1}{2}a_6 v_\eta v_\rho^2 - \frac{\alpha v_\rho v_\chi}{\sqrt{2}}\right), \tag{B.2}$$

$$\mu_3^2 = -\frac{1}{v_\rho}\left(a_3 v_\rho^3 + \frac{1}{2}a_5 v_\rho v_\chi^2 + \frac{1}{2}a_6 v_\eta^2 v_\rho - \frac{\alpha v_\eta v_\chi}{\sqrt{2}}\right). \tag{B.3}$$

Using the identities above we can write the mass matrices for the scalar sector in a simpler form. Here we will present only the eigenvectors from these mass matrices, giving the relationships between symmetry and mass eigenstates and the masses of the particles.

B.1. Double charge scalars

$$\begin{pmatrix}\rho^{++}\\ \chi^{++}\end{pmatrix} = \frac{1}{\sqrt{1+\frac{|v_\chi|^2}{|v_\rho|^2}}}\begin{pmatrix}1 & \frac{|v_\chi|}{|v_\rho|}\\ -\frac{|v_\chi|}{|v_\rho|} & 1\end{pmatrix}\begin{pmatrix}G^{++}\\ Y^{++}\end{pmatrix} \tag{B.4}$$

With masses

$$m_{Y^{++}}^2 = \lambda\left(\frac{1}{|v_\rho|^2}+\frac{1}{|v_\chi|^2}\right) + \frac{a_8}{2}\left(|v_\chi|^2+|v_\rho|^2\right) \tag{B.5}$$

$$m_{G^{++}}^2 = 0 \tag{B.6}$$

where $\lambda = (v_\chi v_\rho v_\eta \alpha)/\sqrt{2}$.

B.2. Single charge scalars

$$\begin{pmatrix} \eta_1^+ \\ \rho^+ \\ \eta_2^+ \\ \chi^+ \end{pmatrix} = \begin{pmatrix} 0 & 0 & -\frac{v_\eta}{\sqrt{\frac{v_\eta^2}{v_\chi^2}+1}v_\chi} & \frac{1}{\sqrt{\frac{v_\eta^2}{v_\chi^2}+1}} \\ \frac{v_\eta C_1-\sqrt{R}}{a_{10}v_\eta^2\left(v_\eta^2+v_\rho^2\right)v_\chi\sqrt{D_1}} & \frac{v_\eta C_1-\sqrt{R}}{a_{10}v_\eta v_\rho\left(v_\eta^2+v_\rho^2\right)v_\chi\sqrt{D_1}} & \frac{2v_\chi}{v_\eta\sqrt{D_1}} & \frac{2}{\sqrt{D_1}} \\ -\frac{v_\eta}{\sqrt{\frac{v_\eta^2}{v_\rho^2}+1}v_\rho} & \frac{1}{\sqrt{\frac{v_\eta^2}{v_\rho^2}+1}} & 0 & 0 \\ \frac{C_1v_\eta+\sqrt{R}}{a_{10}v_\eta^2\left(v_\eta^2+v_\rho^2\right)v_\chi\sqrt{D_2}} & \frac{C_1v_\eta+\sqrt{R}}{a_{10}v_\eta v_\rho\left(v_\eta^2+v_\rho^2\right)v_\chi\sqrt{D_2}} & \frac{2v_\chi}{v_\eta\sqrt{D_2}} & \frac{2}{\sqrt{D_2}} \end{pmatrix} \begin{pmatrix} G_1^+ \\ Y_1^+ \\ G_2^+ \\ Y_2^+ \end{pmatrix} \tag{B.7}$$

where

$$\begin{aligned} R =& v_\eta^2\Big[4a_{10}^2v_\rho^2v_\chi^2\left(v_\eta^2+v_\rho^2\right)\left(v_\eta^2+v_\chi^2\right)+a_7^2v_\rho^2v_\chi^2\left(v_\eta^2+v_\chi^2\right)^2 \\ &-2a_7v_\rho v_\chi\left(v_\eta^2+v_\chi^2\right)\left(a_9v_\rho v_\chi\left(v_\eta^2+v_\rho^2\right)+\sqrt{2}\alpha v_\eta\left(v_\chi^2-v_\rho^2\right)\right)+a_9^2v_\rho^2v_\chi^2\left(v_\eta^2+v_\rho^2\right)^2 \\ &-2\sqrt{2}\alpha a_9v_\eta v_\rho v_\chi\left(v_\eta^2+v_\rho^2\right)(v_\rho-v_\chi)(v_\rho+v_\chi)+2\alpha^2v_\eta^2\left(v_\rho^2-v_\chi^2\right)^2\Big] \end{aligned} \tag{B.8}$$

$$A = a_7v_\eta v_\rho v_\chi\left(v_\eta^2+v_\chi^2\right)+a_9v_\eta v_\rho v_\chi\left(v_\eta^2+v_\rho^2\right)+\sqrt{2}\alpha\left(v_\eta^2\left(v_\rho^2+v_\chi^2\right)+2v_\rho^2v_\chi^2\right) \tag{B.9}$$

$$C_1 = -a_7v_\rho v_\chi\left(v_\eta^2+v_\chi^2\right)+a_9v_\rho v_\chi\left(v_\eta^2+v_\rho^2\right)+\sqrt{2}\alpha v_\eta\left(v_\chi^2-v_\rho^2\right) \tag{B.10}$$

$$C_2 = a_7v_\rho v_\chi\left(v_\eta^2+v_\chi^2\right)-a_9v_\rho v_\chi\left(v_\eta^2+v_\rho^2\right)+\sqrt{2}\alpha v_\eta(v_\rho-v_\chi)(v_\rho+v_\chi) \tag{B.11}$$

$$D_1 = \frac{\left(C_2v_\eta+\sqrt{R}\right)^2}{a_{10}^2v_\eta^2v_\rho^2v_\chi^2\left(v_\eta^2+v_\rho^2\right)^2}+\frac{\left(C_2v_\eta+\sqrt{R}\right)^2}{a_{10}^2v_\eta^4v_\chi^2\left(v_\eta^2+v_\rho^2\right)^2}+\frac{4v_\chi^2}{v_\eta^2}+4 \tag{B.12}$$

$$D_2 = \frac{\left(C_1v_\eta+\sqrt{R}\right)^2}{a_{10}^2v_\eta^2v_\rho^2v_\chi^2\left(v_\eta^2+v_\rho^2\right)^2}+\frac{\left(C_1v_\eta+\sqrt{R}\right)^2}{a_{10}^2v_\eta^4v_\chi^2\left(v_\eta^2+v_\rho^2\right)^2}+\frac{4v_\chi^2}{v_\eta^2}+4 \tag{B.13}$$

with masses

$$m_{Y_1^+}^2 = \frac{A-\sqrt{R}}{4v_\eta v_\rho v_\chi} \tag{B.14}$$

$$m_{Y_2^+}^2 = \frac{A+\sqrt{R}}{4v_\eta v_\rho v_\chi} \tag{B.15}$$

$$m_{G_1^+}^2 = m_{G_2^+}^2 = 0 \tag{B.16}$$

B.3. Neutral scalars

For the CP-odd neutral scalars (the ones that come from the imaginary component of the neutral symmetry eigenstates) we have

$$\begin{pmatrix} I_\eta^0 \\ I_\rho^0 \\ I_\chi^0 \end{pmatrix} = \begin{pmatrix} \frac{N_a}{|v_\chi|} & -\frac{N_b|v_\eta||v_\chi|}{|v_\rho|(|v_\eta|^2+|v_\chi|^2)} & \frac{N_c}{|v_\eta|} \\ 0 & \frac{N_b}{|v_\chi|} & \frac{N_c}{|v_\rho|} \\ -\frac{N_a}{|v_\eta|} & -\frac{N_b|v_\eta|^2}{|v_\rho|(|v_\eta|^2+|v_\chi|^2)} & \frac{N_c}{|v_\chi|} \end{pmatrix} \begin{pmatrix} G_1^0 \\ G_2^0 \\ A^0 \end{pmatrix} \tag{B.17}$$

with masses

$$m_{A^0}^2 = \lambda \left(\frac{1}{|v_\chi|^2} + \frac{1}{|v_\rho|^2} + \frac{1}{|v_\eta|^2} \right) \tag{B.18}$$

$$m_{G_1^0}^2 = m_{G_2^0}^2 = 0 \tag{B.19}$$

where

$$\lambda = (v_\chi v_\rho v_\eta \alpha)/\sqrt{2} \tag{B.20}$$

$$N_a = 1/\sqrt{\frac{1}{|v_\chi|^2} + \frac{1}{|v_\eta|^2}} \tag{B.21}$$

$$N_b = 1/\sqrt{\frac{1}{|v_\chi|^2} + \frac{|v_\eta|^2}{|v_\rho|^2(|v_\eta|^2 + |v_\chi|^2)}} \tag{B.22}$$

$$N_c = 1/\sqrt{\frac{1}{|v_\chi|^2} + \frac{1}{|v_\rho|^2} + \frac{1}{|v_\eta|^2}} \tag{B.23}$$

For the CP-even neutral scalars (which come from the real component of the neutral symmetry eigenstates) it is not possible to find an analytic expression for the mass eigenstates. However, we know that the mass matrix is symmetric, therefore it can be diagonalized by and orthogonal matrix. Therefore, we can write: $X_\psi^0 = \sum_a O_{\psi a}^H H_a^0$, where $\psi = \chi, \eta, \rho$ and $a = 1, 2, 3$. H_a^0 are the mass eigenstates and O^H is an orthogonal matrix. The lightest of the H_a^0 should be the Higgs boson of 125 GeV.

C. Interactions

C.1. Lepton-scalar vertices

In the following equations we denote:

$$\hat{M}^l = \mathrm{diag}(m_e, m_\mu, m_\tau), \quad M^E = diag(m_{E_e}, m_{E_\mu}, m_{E_\tau}), \tag{C.1}$$

with $\nu = (\nu_e, \nu_\mu, \nu_\tau), l = (e, \mu, \tau), E = (E_e, E_\mu, E_\tau)$. The neutral (pseudo)scalars have interactions of the form $\bar{l}(\sqrt{2}\hat{M}^l/v_\rho)l \cdot \sum_{i=1}^{3} O_{\rho i} h_i$, and $\bar{l}(\hat{M}^l/v_\rho)\gamma_5 l \cdot \sum_{i=1}^{3} U_{\rho i} A_i$. Since in this model there is only one physical pseudo-scalar we denote $A_3 \equiv A^0$. Here we have the form factors appearing in Eq. (5.2) (i fixed)

$$S^l_{h_i} = \frac{\sqrt{2}\hat{M}^l}{v_\rho} O_{\rho i}, \quad P^l_A = \frac{\sqrt{2}}{v_\rho^2 \sqrt{\frac{1}{v_\chi^2} + \frac{1}{v_\eta^2} + \frac{1}{v_\rho^2}}} \hat{M}^l U_{\rho 3}. \tag{C.2}$$

The matrix elements $O_{\rho i}$ and $U_{\rho 3}$ relate the symmetry and mass eigenstates, they can be seen in sec. B.3.

For the singly charged scalars $Y^+_{1,2}$, from the Yukawa interactions in Eq. (4.9), the vertex $\bar{\nu}_{iL} E_{jR} Y_1^+$ implies

$$S^l_{Y_1(Y_2)} = P^l_{Y_1(Y_2)} = U_1(U_2) \frac{\sqrt{2}}{v_\rho} (V_L^{l\dagger})_{ij} \hat{M}^l, \tag{C.3}$$

where $U_1(U_2)$ represent the projection of a given singly charged scalar into $Y_{1,2}$. Since the projections are given by complicated expressions involving several unknown constants (see sec. B.2) we have assumed their values to be 0.5. We have explored other values, but there was no noticeable change in our numerical results, given the predominance of the $U^{\pm\pm}$ boson contribution to the AMDM (see sec. 6.2).

Finally, for the doubly charged scalar we have $\bar{l} E Y^{--} \to i(S_Y + \gamma_5 P_Y)$, with

$$\begin{aligned} S_{Y^{--}} &= \frac{\sqrt{2}}{v_\rho} [\cos\alpha \hat{M}^E V_L^{l\dagger} + \sin\alpha V_L^{l\dagger} \hat{M}^l] \\ P^l_{Y^{--}} &= \frac{\sqrt{2}}{v_\rho} [-\cos\alpha \hat{M}^E V_L^{l\dagger} + \sin\alpha V_L^{l\dagger} \hat{M}^l], \end{aligned} \tag{C.4}$$

where $\cos\alpha = v_\rho/\sqrt{v_\rho^2 + v_\chi^2}$ and $\sin\alpha = v_\chi/\sqrt{v_\rho^2 + v_\chi^2}$. where the constants V_S^l and A_S^l are defined in Sec. 4. We assumed that the heavy leptons are in the diagonal basis, $M^E = \hat{M}^E$ and that in (C.4), the v_χ is real, i.e., $\theta_\chi = 0$.

The numerical values for the $V_{L,R}^l$ matrices were obtained in Ref. [34] and [37]. The different sets os matrices considered can be seen in Sec. 6.1.In the interactions above, the matrix V_R^l and the matrix for the Yukawa couplings can always be eliminated by using the mass matrix. The extra factors in the interactions above come from the projection on the SM-like scalars, see [34] for details.

C.2. Scalar-photon vertices

From the lepton Lagrangian we may find the interaction with photon of the known leptons, $l(e\,\mu\,\tau)^T$ and extra leptons $E = (E_e\,E_\mu\,E_\tau)^T$:

$$\mathcal{L}_I = (-e\bar{l}\gamma_\mu l + e\bar{E}\gamma_\mu E)A^\mu \tag{C.5}$$

and identify the electron charge as

$$e = \frac{gt}{\sqrt{1+4t^2}} = gs_W \tag{C.6}$$

where e is the modulus of the electron charge and $t^2 = s_W^2/(1-4s_W^2)$.

Now, from the covariant derivatives of the Lagrangian we can find the vertices for the interactions between scalars and photons:

$$\begin{aligned} &A_\mu Y^{++}Y^{--} \to i2e(k^- - k^+)_\mu, \quad A_\mu Y_2^+ Y_2^- \to ie(k^- - k^+)_\mu, \\ &A_\mu Y_1^+ Y_1^- \to ie(k^- - k^+)_\mu. \end{aligned} \tag{C.7}$$

The terms k^+ and k^- indicate, respectively, the momenta of the positive and negative charge scalars, and both should be considered incoming into the vertex.

C.3. Gauge vertices

For three gauge bosons denoted generically by X, Y and Z, with all momenta incoming (denoted by k), the vertex is:

$$X_\nu Y_\lambda Z_\mu \to iG_{XYZ}\left[g_{\nu\lambda}\left(k^X - k^Y\right)_\mu + g_{\lambda\mu}\left(k^Y - k^Z\right)_\nu + g_{\mu\nu}\left(k^Z - k^X\right)_\lambda\right] \tag{C.8}$$

The proportionality constants are:

$$G_{WWA} = e, \quad G_{VVA} = -e, \quad G_{UUA} = -2e, \quad G_{WWZ} = -e/t_W,$$
$$G_{WWZ'} = 0, G_{VVZ} = -\frac{e}{2}\left(\frac{1}{t_W} + 3t_W\right), \quad G_{VVZ'} = e\frac{\sqrt{3}}{2}\frac{\sqrt{1-4s_W^2}}{s_W c_W},$$
$$G_{UUZ} = \frac{e}{2}\left(\frac{1}{t_W} - 3t_W\right), G_{UUZ'} = e\frac{\sqrt{3}}{2}\frac{\sqrt{1-4s_W^2}}{s_W c_W}. \tag{C.9}$$

where s_W, c_W and t_W are, respectively, the sine, cosine and tangent of the weak mixing angle, θ_W.

C.4. Charged gauge-lepton interactions

The Lagrangian terms for interactions among charged gauge bosons and leptons may be written as follows:

- ν-type and l-type leptons:

$$\mathcal{L}_{\nu l} = \frac{g}{2\sqrt{2}}\bar{\nu}_i\gamma^\mu\left(1-\gamma_5\right)\left(V_{PMNS}\right)_{ij}l_j W_\mu^+ + H.c. \tag{C.10}$$

  for $i = 1, 2, 3$ and $j = 1, 2, 3$ and V_{PMNS} is the Pontecorvo-Maki-Nagaoka-Sakata matrix.

- E-type and ν-type leptons:

$$\mathcal{L}_{E\nu} = \frac{g}{2\sqrt{2}}\bar{E}_i\gamma^\mu\left(1-\gamma_5\right)\left(U_L^\nu\right)_{ij}\,\nu_j\,V_\mu^+ + H.c. \tag{C.11}$$

  for $i = 1, 2, 3$. U_L^ν is the unitary matrix relating the neutrino symmetry eigenstates with the mass eigenstates. We also assume that the heavy leptons are in the diagonal basis.

- E-type and l-type leptons:

$$\mathcal{L}_{El} = \frac{g}{2\sqrt{2}}\bar{E}_i\gamma^\mu\left(1-\gamma_5\right)\left(V_L^{l\dagger}\right)_{ij}l_j U_\mu^{++} + H.c. \tag{C.12}$$

  for $i, j = 1, 2, 3$ and V_L^l is given in Sec. 6.1. Notice that in this model

$$V_U^l = A_U^l = \frac{g}{2\sqrt{2}}V_L^{l\dagger}, \tag{C.13}$$

  .

C.5. Neutral gauge-lepton interactions

Considering the following Lagrangian for the neutral interactions:

$$\mathcal{L}_{NC} = -\frac{g}{2c_W}\sum_i \bar{\psi}_i\gamma^\mu\left[\left(g_V^i - g_A^i\gamma_5\right)Z_\mu + \left(f_V^i - f_A^i\gamma_5\right)Z'_\mu\right]\psi_i \tag{C.14}$$

where ψ_i can be any lepton mass eigenstate, we find the g_V^i, g_A^i, f_V^i and f_A^i to be:

$$\begin{aligned} &g_V^\nu = \frac{1}{2}, \quad g_A^\nu = \frac{1}{2}, \quad g_V^l = -\frac{1}{2} + s_W^2, \quad g_A^l = -\frac{1}{2} + s_W^2, \\ &g_V^E = g_A^E = -s_W^2, \end{aligned} \tag{C.15}$$

$$\begin{aligned} f_V^\nu &= -\frac{\sqrt{1-4s_W^2}}{2\sqrt{3}}, \quad f_A^\nu = -\frac{\sqrt{1-4s_W^2}}{2\sqrt{3}} \\ f_V^l &= -\frac{\sqrt{1-4s_W^2}}{2\sqrt{3}}, \quad f_A^l = -\frac{\sqrt{1-4s_W^2}}{2\sqrt{3}}, \\ f_V^E &= \frac{\sqrt{1-4s_W^2}}{2\sqrt{3}}, \quad f_A^E = \frac{\sqrt{1-4s_W^2}}{2\sqrt{3}} \end{aligned} \tag{C.16}$$

D. Scalar-fermion loop diagram calculation

As an example of the calculations performed to find the AMDM from the diagrams presented in Fig. 5.2, we will show some of the details in the calculation of diagram a) of the mentioned figure, where we have a scalar-fermion loop with the photon connected to the fermion.

Remembering that $q = p' - p$ and that k is the momentum to be integrated in the loop, and also using, from the Feynman parametrization, $l = k + yq - zp$, the diagram can be written as

$$\Gamma^{\mu} = 2i \int d^4k dx dy dz \left[\bar{u}(p') \frac{N^{\mu}}{D^3} u(p) \right] \delta(x + y + z - 1); \tag{D.1}$$

where

$$N^{\mu} = (S + A\gamma_5)(\not{k} + m_I)(Q\gamma^{\mu})(\not{k} + \not{q} + m_I)(S^{\dagger} + P^{\dagger}\gamma_5), \tag{D.2}$$

$$D = l^2 - m_I^2(1 - z) + q^2 xy + m_l^2 z(1 - z) - zM^2, \tag{D.3}$$

being Q the electric charge of the fermion in the loop, m_I the mass of the fermion in the loop, m_l the mass of the external fermion, S and P the scalar and pseudoscalar vertices and M the mass of the scalar.

To proceed, we expand the numerator N in Eq. D.1 - remembering that we have $\bar{u}(p')N^{\mu}u(p)$ - and perform the following substitutions in the presented order:

- $\not{k} \to \not{l} + \not{p}z - \not{q}y$;
- $\not{q} \to \not{p}' - \not{p}$;
- $\gamma_5 \not{p} \gamma^{\mu} \not{p} \gamma_5 \to -\not{p} \gamma^{\mu} \not{p}$;
- $\gamma_5 \not{p} \gamma^{\mu} \not{p}' \gamma_5 \to -\not{p} \gamma^{\mu} \not{p}'$;
- $\gamma_5 \not{p}' \gamma^{\mu} \not{p} \gamma_5 \to -\not{p}' \gamma^{\mu} \not{p}$;
- $\gamma_5 \not{p}' \gamma^{\mu} \not{p}' \gamma_5 \to -\not{p}' \gamma^{\mu} \not{p}'$;

- $\not{p}\gamma^\mu\not{p} \to 2p^\mu\not{p} - \gamma^\mu m_l^2$;
- $\not{p}'\gamma^\mu\not{p}' \to 2p'^\mu\not{p}' - \gamma^\mu m_l^2$;
- $\not{p}\gamma^\mu\not{p}' \to \gamma^\mu(q^2 - 2m_l^2) - \not{p}'\gamma^\mu\not{p} + p^\mu\not{p}' + 2p'^\mu\not{p}$;
- $\gamma^\mu\not{p}' \to 2p'^\mu - \not{p}'\gamma^\mu$;
- $\not{p}\gamma^\mu \to 2p^\mu - \gamma^\mu\not{p}$;
- $\not{p}'\gamma^\mu\not{p}\gamma_5 \to -m_l^2\gamma^\mu\gamma_5$;
- $\gamma_5\not{p}'\gamma^\mu\not{p} \to -m_l^2\gamma_5\gamma^\mu$;
- $\gamma_5\not{p}'\gamma^\mu\gamma_5 \to \gamma^\mu m_l$;
- $\gamma_5\gamma^\mu\not{p}\gamma_5 \to \gamma^\mu m_l$;
- $\not{p}'\gamma^\mu\not{p} \to \gamma^\mu m_l^2$;
- $\not{p}'\gamma^\mu\gamma_5 \to m_l\gamma^\mu\gamma_5$;
- $\gamma^\mu\not{p}\gamma_5 \to -m_l\gamma^\mu\gamma_5$;
- $\gamma_5\not{p}'\gamma^\mu \to m_l\gamma^\mu\gamma_5$;
- $\gamma_5\gamma^\mu\not{p} \to -m_l\gamma^\mu\gamma_5$;
- $\not{p}\gamma_5 \to \gamma_5(-m_l)$;
- $\not{p}'\gamma^\mu \to \gamma^\mu m_l$;
- $\not{p}'\gamma_5 \to \gamma_5 m_l$;
- $\gamma^\mu\not{p} \to \gamma^\mu m_l$;
- $\gamma_5\not{p} \to \gamma_5 m_l$;
- $\gamma_5\not{p}' \to \gamma_5(-m_l)$;
- $\gamma_5\gamma^\mu \to -\gamma^\mu\gamma_5$;
- $\gamma_5\gamma_5 \to 1$;
- $\not{p} \to m_l$;

- $\not{p}' \to m_l$.

It is important the follow the order above to ensure that we have all $\not{p}'$ on the left and all $\not{p}$ on the right, so we can use the identities $\bar{u}(p')\not{p}' = m_l$ and $\not{p}u(p) = m_l$. After these substitutions, we use Gordon's identity (Eq. 2.27), take the terms proportional to $i\sigma_{\mu\nu}q^\nu/2m_l$, and perform the integrations (using the identities shown in Sec 2.1). Doing so should lead to

$$\Delta a = \int_0^1 dz \frac{m_l Q(z(|P|^2(m_l(z-1)+m_I)+|S|^2(m_l(-z)+m_l+m_I)))}{8\pi^2\left(m_I^2 z - M^2(z-1)\right)}. \tag{D.4}$$

The above equation can then be rearranged to match the equation in Sec. 5.1.

Bibliography

[1] K. A. Olive *et al.* [Particle Data Group Collaboration], Review of Particle Physics, Chin. Phys. C **38**, 090001 (2014).

[2] T. Aoyama, M. Hayakawa, T. Kinoshita and M. Nio, Tenth-Order Electron Anomalous Magnetic Moment — Contribution of Diagrams without Closed Lepton Loops, Phys. Rev. D **91**, no. 3, 033006 (2015) [arXiv:1412.8284 [hep-ph]].

[3] F. Jegerlehner and A. Nyffeler, The Muon g-2 Phys. Rept. **477**, 1 (2009) [arXiv:0902.3360 [hep-ph]].

[4] J. P. Miller, E. d. Rafael, B. L. Roberts and D. Stckinger, Muon (g-2): Experiment and Theory, Ann. Rev. Nucl. Part. Sci. **62**, 237 (2012).

[5] T. Blum, A. Denig, I. Logashenko, E. de Rafael, B. Lee Roberts, T. Teubner and G. Venanzoni, The Muon (g-2) Theory Value: Present and Future, arXiv:1311.2198 [hep-ph].

[6] C. Kelso, P. R. D. Pinheiro, F. S. Queiroz and W. Shepherd, The Muon Anomalous Magnetic Moment in the Reduced Minimal 3-3-1 Model, Eur. Phys. J. C **74**, 2808 (2014) [arXiv:1312.0051 [hep-ph]].

[7] A. Dias, J. Montero, V. Pleitez. Closing the $SU(3)_L \otimes U(1)_X$ symmetry at the electroweak scale. Phys. Rev. D **73**(11), 113004 (2006)

[8] C. Kelso, H. N. Long, R. Martinez and F. S. Queiroz, Connection of $g-2_\mu$, electroweak, dark matter, and collider constraints on 331 models, Phys. Rev. D **90**, no. 11, 113011 (2014) [arXiv:1408.6203 [hep-ph]].

[9] N. A. Ky, H. N. Long and D. V. Soa, Anomalous magnetic moment of muon in 3 3 1 models, Phys. Lett. B **486**, 140 (2000) [hep-ph/0007010];

[10] D. T. Binh, D. T. Huong and H. N. Long, Muon anomalous magnetic moment in the supersymmetric economical 3-3-1 model, Zh. Eksp. Teor. Fiz. **148**, 1115 (2015) [J. Exp. Theor. Phys. **121**, no. 6, 976 (2015)]; [arXiv:1504.03510 [hep-ph]].

[11] J. H. Taibi and N. Mebarki, Muon Anomalous Magnetic Moment in the Left-Right Symmetric Model, J. Phys. Conf. Ser. **593**, no. 1, 012017 (2015).

[12] D. Chowdhury and N. Yokozaki, Muon $g-2$ in anomaly mediated SUSY breaking, JHEP **1508**, 111 (2015); [arXiv:1505.05153 [hep-ph]].

[13] K. Harigaya, T. T. Yanagida and N. Yokozaki, Muon $g-2$ in focus point SUSY, Phys. Rev. D **92**, no. 3, 035011 (2015); [arXiv:1505.01987 [hep-ph]].

[14] M. A. Ajaib, B. Dutta, T. Ghosh, I. Gogoladze and Q. Shafi, Neutralinos and sleptons at the LHC in light of muon $(g-2)_\mu$, Phys. Rev. D **92**, no. 7, 075033 (2015); [arXiv:1505.05896 [hep-ph]].

[15] B. P. Padley, K. Sinha and K. Wang, Natural Supersymmetry, Muon $g-2$, and the Last Crevices for the Top Squark, Phys. Rev. D **92**, no. 5, 055025 (2015); [arXiv:1505.05877 [hep-ph]].

[16] S. Khalil and C. S. Un, Muon Anomalous Magnetic Moment in SUSY B-L Model with Inverse Seesaw, arXiv:1509.05391 [hep-ph].

[17] T. Abe, R. Sato and K. Yagyu, Lepton-specific two Higgs doublet model as a solution of muon $g-2$ anomaly, JHEP **1507**, 064 (2015); [arXiv:1504.07059 [hep-ph]].

[18] E. J. Chun, Limiting two-Higgs-doublet models, arXiv:1505.00491 [hep-ph] (2015) (unpublished).

[19] A. J. Buras, F. De Fazio, J. Girrbach and M. V. Carlucci, The Anatomy of Quark Flavour Observables in 331 Models in the Flavour Precision Era, JHEP **1302**, 023 (2013); [arXiv:1211.1237 [hep-ph]].

[20] A. J. Buras, F. De Fazio and J. Girrbach-Noe, Z-Z' mixing and Z-mediated FCNCs in $SU(3)_C \times SU(3)_L \times U(1)_X$ models, JHEP **1408**, 039 (2014); [arXiv:1405.3850 [hep-ph]].

[21] A. J. Buras, The Renaissance of Kaon Flavour Physics, arXiv:1606.06735 [hep-ph].

[22] R. Martinez, F. Ochoa and C. F. Sierra, Diphoton decay for a 750 GeV scalar boson in an $U(1)'$ model, arXiv:1512.05617 [hep-ph].

[23] A. E. C. Hernández and I. Nisandzic, LHC diphoton 750 GeV resonance as an indication of $SU(3)_c \times SU(3)_L \times U(1)_X$ gauge symmetry, arXiv:1512.07165 [hep-ph].

[24] Q. H. Cao, Y. Liu, K. P. Xie, B. Yan, and D. M. Zhang, Diphoton excess, low energy theorem, and the 331 model, Phys. Rev. D **93**, no. 7, 075030 (2016) [arXiv:1512.08441 [hep-ph]]

[25] R. Martinez, F. Ochoa and C. F. Sierra, $\boldsymbol{SU(3)_C \otimes SU(3)_L \otimes U(1)_X}$ models in view of the 750 GeV diphoton signal, arXiv:1606.03415 [hep-ph].

[26] J. de Blas, J. Santiago and R. Vega-Morales, New vector bosons and the diphoton excess, Phys. Lett. B **759**, 247 (2016) [arXiv:1512.07229 [hep-ph]].

[27] G. De Conto and V. Pleitez, Phys. Rev. D **96**, no. 7, 075028 (2017) doi:10.1103/PhysRevD.96.075028 [arXiv:1708.06285 [hep-ph]].

[28] J. D. Bjorken and C. H. Llewellyn Smith, Spontaneously Broken Gauge Theories of Weak Interactions and Heavy Leptons, Phys. Rev. D **7**, 887 (1973).

[29] J. R. Primack and H. R. Quinn, Muon g-2 and other constraints on a model of weak and electromagnetic interactions without neutral currents, Phys. Rev. D **6**, 3171 (1972).

[30] G. De Conto and V. Pleitez, Electron and muon anomalous magnetic dipole moment in a 331 model, JHEP **1705**, 104 (2017).

[31] V. Pleitez and M. D. Tonasse, Heavy charged leptons in an $SU(3)_L \otimes U(1)_N$ model, Phys. Rev. D **48**, 2353 (1993) [hep-ph/9301232].

[32] W. Bernreuther, M. Suzuki. The electric dipole moment of the electron. Rev. Mod. Phys. **63**(2), 313-340 (1991).

[33] M. E. Peskin, D. V. Schroeder. An Introduction to Quantum Field Theory. Addison-Wesley (1995).

[34] G. De Conto and V. Pleitez, Electron and neutron electric dipole moment in the 3-3-1 model with heavy leptons, Phys. Rev. D **91**, 015006 (2015); [arXiv:1408.6551 [hep-ph]].

[35] A. C. B. Machado, J. C. Montero, V. Pleitez, FCNC in the minimal 3-3-1 model revisited, Phys. Rev. D **88**, 113002 (2013); [arXiv:1305.1921 [hep-ph]].

[36] J. C. Montero and B. L. Sanchez-Vega, Natural PQ symmetry in the 3-3-1 model with a minimal scalar sector, Phys. Rev. D **84**, 055019 (2011); [arXiv:1102.5374 [hep-ph]].

[37] A. C. B. Machado, J. Monta no and V. Pleitez, Lepton number violating processes in the minimal 3-3-1 model with singlet sterile neutrinos, arXiv:1604.08539 [hep-ph].

[38] G. De Conto, A. C. B. Machado and V. Pleitez, Minimal 3-3-1 model with a spectator sextet, Phys. Rev. D **92**, no. 7, 075031 (2015); [arXiv:1505.01343 [hep-ph]].

[39] V. Pleitez and M. D. Tonasse, Neutrinoless double beta decay in an $SU(3)_L \otimes U(1)_N$ model, Phys. Rev. D **48**, 5274 (1993); [hep-ph/9302201].

[40] E. J. Konopinski and H. M. Mahmoud, The Universal Fermi interaction, Phys. Rev. **92**, 1045 (1953).

[41] J. C. Montero, V. Pleitez and O. Ravinez, Soft superweak CP violation in a 331 model, Phys. Rev. D **60**, 076003 (1999) [hep-ph/9811280].

[42] A. G. Dias, J. C. Montero, V. Pleitez, Closing the $SU(3)_L \otimes U(1)_X$ symmetry at electroweak scale, Phys. Rev. D **73**, 113004 (2006); [hep-ph/0605051].

[43] A. G. Dias, R. Martinez and V. Pleitez, Concerning the Landau pole in 3-3-1 models, Eur. Phys. J. C **39** (2005) 101 [hep-ph/0407141].

[44] J. T. Liu and D. Ng, Lepton flavor changing processes and CP violation in the 331 model, Phys. Rev. D **50**, 548 (1994) [hep-ph/9401228].

[45] W. H. Bertl *et al.* [SINDRUM II Collaboration], A Search for muon to electron conversion in muonic gold, Eur. Phys. J. C **47** (2006) 337.

[46] C. A. de S.Pires and P. S. Rodrigues da Silva, Scalar scenarios contributing to $(g-2)_\mu$ with enhanced Yukawa couplings, Phys. Rev. D **64**, 117701 (2001); [hep-ph/0103083];

[47] M. C. Gonzalez-Garcia, M. Maltoni, J. Salvado and T. Schwetz, Global fit to three neutrino mixing: critical look at present precision, JHEP **1212**, 123 (2012); [arXiv:1209.3023 [hep-ph]].